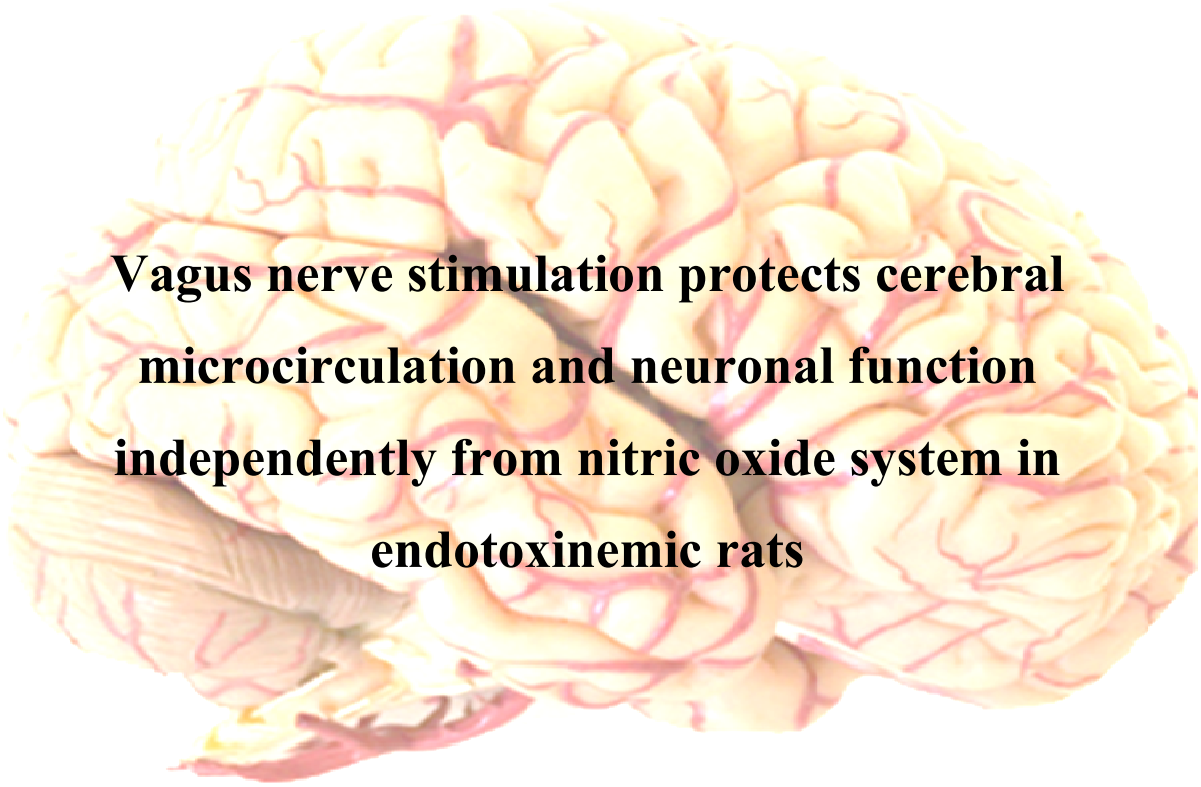

Vagus nerve stimulation protects cerebral microcirculation and neuronal function independently from nitric oxide system in endotoxinemic rats

INAUGURAL-DISSERTATION

zur Erlangung des Grades eines Doktors der Humanbiologie

des Fachbereichs Medizin

der Justus-Liebig-Universität Giessen

vorgelegt von

Mihaylova Stanka

Tierärztin aus Smolyan/Bulgarien

Giessen 2013

Aus der Klinik für Neurologie
Universitätsklinikum Giessen und Marburg GmbH
Standort Giessen

Gutachter: Prof. Dr. B. Rosengarten

Gutachter: Prof. Dr. W. Kummer

Tag der Disputation: 05.02.2013

To My Mother

INDEX

1. INTRODUCTION

1.1. Sepsis

1.1.1. Incidence of sepsis

Sepsis and SIRS (systemic inflammatory response syndromes) are the leading causes of death in intensive care units (ICUs). In industrialized countries, it has an average incidence of 300/100.000 per year, increasing significantly in the elderly (Martin, Mannino et al. 2003; Engel, Brunkhorst et al. 2007). Despite many improvements in ICU patient therapy, there is still no effective therapy for sepsis, outside of the classic catecholamine therapy, which however does not decrease the lethality of sepsis-patients; which lies between 40 and 70% (Bolton, Young et al. 1993). In the United States, approximately 600.000 patients develop sepsis per year and about 240.000 of these patients will succumb to the disease (Angus, Linde-Zwirble et al. 2001). Due to the smaller total population number, the number of sepsis and SIRS incidences in Germany is about a quarter of those in the USA (Engel, Brunkhorst et al. 2007). Reasons for the rise of sepsis cases are both that patients grow older and that the number of patients with immunodeficiency is increasing. Whether increasing resistance of microorganisms is a contributing factor is still in debate.

1.1.2. Definition of sepsis

Though the term sepsis is linked closely to modern intensive care, the medical concept is rather older. The word "sepsis" was first introduced by Hippocrates (ca. 460-370 BC) and is derived from the Greek word sipsi ("make rotten"). Ibn Sina (979-1037 BC) observed the coincidence of blood putrefaction (septicaemia) and fever. This concept of sepsis which was introduced in classical antiquity was used until the 19th century. In 1914, Schottmüller gave a clinical definition of sepsis: Sepsis occurs in cases of permanent or periodical invasion of pathogenic germs into the blood circulation (Schottmüller 1914). Later in 1980, sepsis was defined as the release of humoral and cellular mediators from the host by Schuster and Werdan (Schuster HP 2005).

In 1991, a consensus conference held by the American College of Chest Physicians (ACCP) and the Society of Critical Care Medicine (SCCM) took place with the aim of agreeing on a set of definitions that could be applied to patients with sepsis and its sequelae. This concept is used mainly by clinicians and researchers for the purposes of

clinical trial design for more than 20 years now (Bone, Balk et al. 1992). Some definitions of this concept are given below.

SIRS is defined by a variety of severe clinical insults such as trauma, burns, and pancreatitis. The response is manifested by two or more of the following conditions of systemic inflammation: fever or hypothermia (temperature >38°C or <36°C), tachycardia (heart rate >90 beats/min without hypovolemia), and tachypnea or a supranormal minute ventilation (respiratory rate >20 breaths/min or $PaCO_2$ <32mmHg), leukocytosis or leucopenia (WBC >12.000 cells/nl, <4.000 cells/nl, or >10% immature (band) forms). Sepsis is defined as a systemic inflammatory response syndrome (SIRS) plus a documented infection**.** Severe sepsis however is defined as sepsis with organ dysfunction, hypoperfusion or hypotension. Another term, "septic shock" indicates severe sepsis with hypotension, despite adequate fluid resuscitation. Infection/Bacteraemia describes an infection, which does not meet SIRS conditions. Multiple Organ Dysfunction Syndrome (MODS) occurs by altered organ function in an acutely ill patient such that homeostasis cannot be maintained without intervention.

Though SIRS presents the clinical manifestation of released pro-inflammatory cytokines in the early stage of inflammation, this could also occur by non-infectious processes such as drug reaction and overdose. This makes the SIRS concept not specific for sepsis. An alternative to this concept was developed, in 2001 at the International Sepsis Definitions Conference providing a practical frame for defining the systemic inflammation caused by infection. They created the so-called PIRO concept which combines and analyzes different stages of sepsis by four criteria: predisposition, infection, response to the infectious challenge, and organ dysfunction (Howell, Talmor et al. 2011). Although these definitions have proved valuable, it is still difficult to systematically stage the severity of sepsis.

1.1.3. Pathophysiology of sepsis

1.1.3.1. General aspects

1.1.3.1.1. General aspects of immune response

Although the body is constantly being exposed to microbes, it does not develop inflammation, because of both its physical and chemical barriers as well as its immune system. Physical barriers include the skin, mucous membranes, tears, earwax, mucus, and stomach acid. Usually, the skin prevents invasion from microorganisms unless it is damaged by an injury, insect bite, or burn. Other effective physical barriers are the mucous membranes, such as the linings of the mouth, nose, and eyelids. Mucous membranes are coated with secretions that fight against microorganisms. For example, the mucous membranes of the eyes are bathed in tears, which contain an enzyme called lysozyme that attacks bacteria and protects the eyes from infection. Enzymes and pH are examples of chemical barriers. Microorganisms in the air become bound to the mucus of the nose, which are coughed up or blown out. The digestive tract has a series of effective barriers, including stomach acid, pancreatic enzymes, bile, and intestinal secretions.

The immune system protects the body from infection through both general and specific components. The innate immune system is the more general component of the immune system and is present even before the onset of infection. It consists of disease-resistance mechanisms that are not specific to particular pathogens, but induce the release of cellular and molecular components that recognize classes of molecules. This is because it either uses mechanisms or cells as well as molecules that become active within minutes of exposure to microbial pathogens such as gram-negative organisms (e.g. Escherichia coli, (lipopolysaccharide=LPS), and Pseudomonas aeruginosa) or gram-positive organisms (e.g. lipoteichoic acid, Streptococcus pneumoniae), as well as fungal (e.g. Aspergillus fumigates), viral, and parasitic components. However, the immune system reacts against these pathogens only after recognition of pathogen components by innate receptors that are expressed on immune and non-immune cells. TLRs (Toll-like receptors), RLRs [RIG-I (retinoic acid-inducible gene-I)-like receptors], NLRs (Nod-like receptors) and C-type lectin receptors are specific to the innate immune response. These so called “innate pattern recognition receptors” (PRRs) are able to identify pathogens or their activated products in different cellular parts, such as the plasma membrane or the cytoplasm. Toll-like receptor 2 (TLR2) recognizes lipoteichoic acid

from gram-positive bacteria and toll-like receptor 4 (TLR4) lipopolysaccharide (LPS) from gram-negative germs, which is thought to be an important trigger of the inflammatory response in sepsis. Next come the macrophages and dendritic cells, which phagocytize the pathogen, or induce the expression of cytokines, chemokines and co-stimulatory molecules. Non-immune cells such as epithelial cells, endothelial cells, and fibroblasts also contribute to the innate immune system.

Innate responses trigger the activation of long-lasting pathogen-specific adaptive immune responses. Adaptive immunity is capable of recognizing and selectively eliminating specific foreign microorganisms and molecules. Adaptive immune responses are not the same in all members of a species. Adaptive immunity is determined by the unique set of reactions to specific antigenic challenges that the organism has incurred over its lifetime. Adaptive immunity therefore has four characteristic attributes: antigenic specificity, diversity, immunologic memory, self/non-self recognition.

B- and T-cells belong to the adaptive immune system, and both arise in the bone marrow. B-cells produce pathogen-specific antibodies which eliminate the toxin. They are divided into memory B cells and effector B cells called plasma cells. Memory B cells express the same membrane-bound antibody as their parent B cell. Plasma cells produce the antibody in a form that can be secreted and have little or no membrane-bound antibody. Although plasma cells live for only a few days, they secrete enormous amounts of antibody during this time. Secreted antibodies are the major effector molecules of humoral immunity. T-cell receptors can recognize only antigens that are bound to cell-membrane proteins which make up the major histocompatibility complex (MHC) molecules. There are subpopulations of T cells: T helper (T_H) and T cytotoxic (T_C) cells and T suppressor (T_S) cell. After a T_H cell recognizes and interacts with an antigen–MHC complex, the cell is activated and becomes an effector cell that secretes various growth factors known as cytokines. The secreted cytokines play an important role in activating B cells, T_C cells, macrophages, and various other cells that participate in the immune response (Kindt, Osborne et al. 2000; Rittirsch, Flierl et al. 2008; Kumar, Kawai et al. 2009; Takeuchi and Akira 2010) (Figure 1).

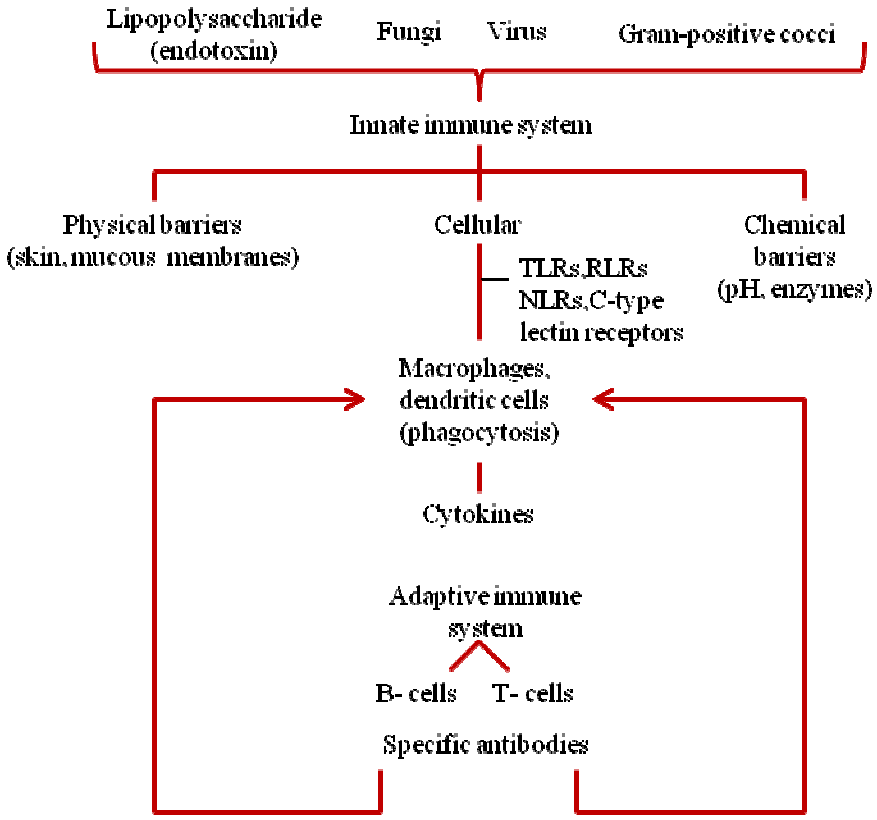

Figure 1. Immune system response to pathogenic germs. TLRs Toll-like receptors, RLRs [RIG-I (retinoic acid-inducible gene-I)-like receptors], NLRs (Nod-like receptors) and C-type lectin receptors (Modified from Kindt, Osborne et.al. 2000).

Cytokines play an important role in the pathogenesis of sepsis, because of their regulatory impact on cell death of inflamed tissues, modification of vascular endothelial permeability, and the recruiting of blood cells to the site of inflammation. Leukocytes, endothelial cells and other immune cells synthesize cytokines. They are a group of polypeptide hormones, which affect different target cells and are part of a complex network. Nuclear factor-κB (NF-κB) regulates the expression of cytokines and is involved in the immune response through T-cell and B-cell receptors. NF-κB signaling leads to a production of pro-inflammatory cytokines such as tumor necrosis factor α (TNF-α) and interleukin 6 (IL-6). During early sepsis, a hyper-inflammatory reaction comprised of the release of TNF-α, IL-6 and interferon ɣ (IFN-ɣ), so-called immune stimulation, is observed. Following the hyper-inflammatory response, the body responds with a compensatory reaction by producing anti-inflammatory cytokines such

as interleukin 10 (IL-10), which then leads to a hypo-inflammatory state, or so-called immune paralysis. Despite the linear occurrence of the immune reaction, there is also a close cross talk between the innate and adaptive immune system (Seeger and Walmrath 2005; Takeuchi and Akira 2010) (Figure 2).

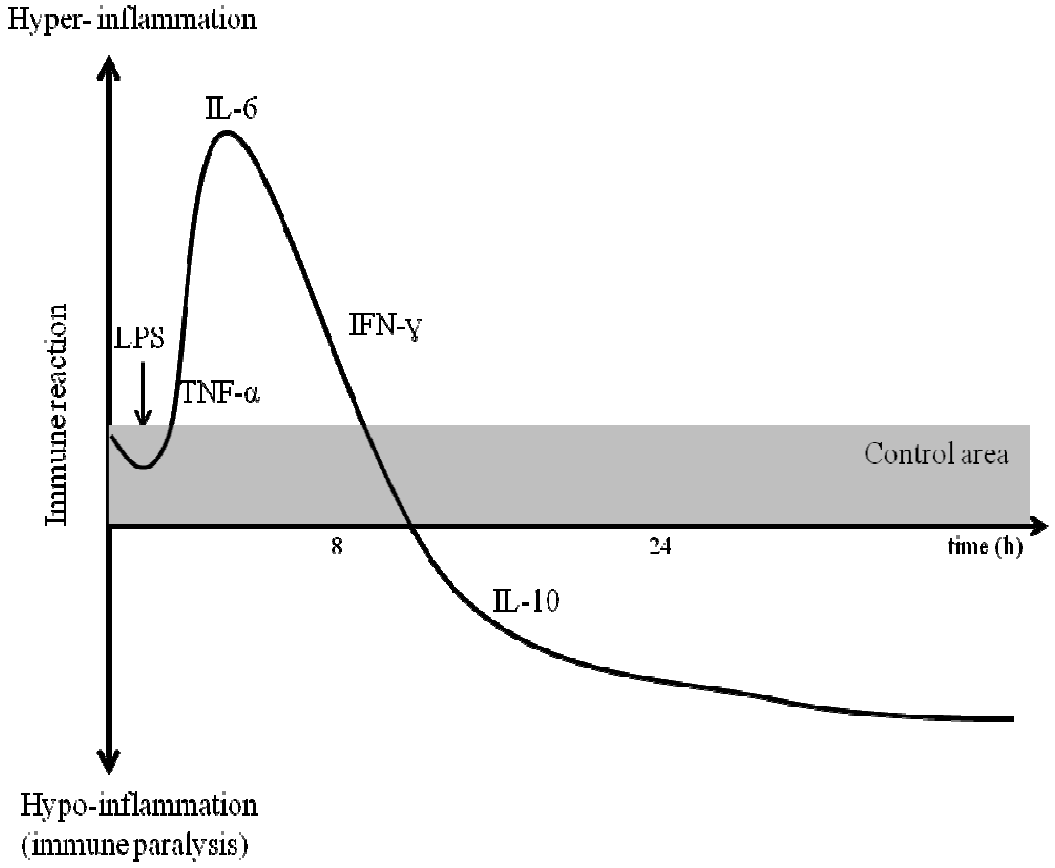

Figure 2. Hypothetical timing of immune reaction to sepsis (Modified from Seeger and Walmrath 2005).

The general effect of TNF-α is based on the inhibition of lipoprotein lipase activity, which induces cachexia. It is responsible for induction of other cytokines such as IL-1, IL-6 and IL-8. In addition, it increases the adherence of granulocytes (PMN-polymorphonuclear leukocytes) to endothelial cells by endothelial and granulocytic reactions. The cells are activated and the vascular diapedesis of PMNs into surrounding tissues is increased. Increased TNF-levels are the reason for the occurrence of the first cardinal signs of acute inflammation described by Celsus: Dolor (pain), Calor (heat), Rubor (redness), Tumor (swelling) and Functio laesa (loss of function) (Yale University. Dept. of the History of Science and Medicine and Yale University. Dept. of the History of Medicine. 1946; Tracy 2006). TNF-α sensitizes the endothelium for the

coagulation cascade and induces a variety of secondary inflammatory mediators such as prostaglandins, thromboxane, leuktriene, NO and reactive oxygen.

IL-6 production leads to the release of acute-phase proteins by hepatocytes. Some authors even suggest its role as an early prognostic parameter for sepsis outcome. In experimentally induced sepsis models, it is possible to obtain plasma measurements of TNF-α and then IL-6 after initial stimulation due to the regulated release of cytokines. After cell come in contact with LPS, mononuclear cells release first TNF-α, which leads to formation, and release of IL-6 and by autocrine feedback further release of TNF-α. Therefore, in this case, IL-6 is responsible for the autocrine feedback of TNF-α.

IFN-γ, or type II interferon, belongs also to the cytokine family. It is also known as the primary "macrophage-activating factor" and plays a greater role in the maturation and function of both innate immune system and adaptive immune system cells. In addition, IFN-γ plays a critical role in shaping the host adaptive T-cell and B-cell response. IFN-γ can be considered as a broad immune mediator involved in activating and directing the host immune response to infection. Moreover it has immunostimulatory as well as immunomodulatory effects. The cytokine IL-10 inhibits the release of pro-inflammatory cytokines from monocytes and macrophages and the formation of inducible NO synthase (iNOS). These effects characterize IL-10 as a potent immunosuppressive cytokine (Seeger and Walmrath 2005; Gamero et al. 2006).

1.1.3.1.2. General aspects of nitric oxide

NO is believed to play a key role in the pathophysiology of sepsis. It is derived from the enzymatic oxidation of L-arginine by NO synthases (NOS) family of enzymes. There exists three isoforms of NOS: endothelial (eNOS) and neuronal NOS (nNOS), which are involved in homeostasis and an inducible form (iNOS). iNOS is mainly expressed in inflamed areas. Endotoxin and cytokines such as TNF-α and IL-6 induce and regulate the synthesis of NO from endothelial cells. The resulting arterial hypotension is a characteristic property of NO by septic shock. Under septic conditions NO concentration increases substantially; 100 to 1000-fold higher than the normal physiological concentration. These excessive increased NO-levels overwhelm the compensatory vasoconstrictive mechanisms (Iadecola 1993; Linehan, Kolios et al. 2005).

1.1.3.1.3. General aspects of microcirculation as a motor of sepsis organ dysfunction

Since 2005 there has been growing evidence that the microcirculation plays an important role in sepsis related organ dysfunction. In previous studies it has been shown that a microcirculatory failure appears before the collapse of the systemic macrocirculation. For example, lactate levels increased drastically despite persistent blood pressure levels (Lehr et al. 2000; Rosengarten, Hecht et al. 2007). Clinically, it has been demonstrated that diagnosis and treatment during the early phase of sepsis; the first 6 to 24 hours, are relevant for determining patient prognosis. During this early phase, acute activation of the innate immune response occurs, otherwise known as a "cytokine storm" resulting in increased NO levels which are related to progressive microcirculatory failure (Hotchkiss, Coopersmith et al. 2009; Lundy and Trzeciak 2009).

Microcirculation includes the capillaries or the smallest units or segments of the circulatory system. Endothelial cells, smooth muscle cells, as well as the constantly changing pool of circulating blood cells are affected during sepsis (Figure 3). Exaggerated production of pro-inflammatory cytokines and the induction of more mediators such as NO and prostaglandins (PGEs) have been implicated in the endothelial activation or dysfunction, an increase in microvascular permeability, endothelial-leukocyte adhesion with uncontrolled cell infiltration and vasodysregulation resulting in peripheral vascular resistance. These vasoactive mediators cause inappropriate vasodilation, hypovolemia, and myocardial depression. Vasodilation further decreases cardiac pre-load because of diminished venous return. This causes changes to occur in the shape of blood cells and capillaries as well as vasoplegia and misdistribution of blood flow on a microvascular level, associated with tissue hypoxia. Due to the damage of the blood vessels endothelial cells, an increase of capillary permeability (capillary leakage syndrome) results, which is responsible for the breakdown of endothelial and epithelial barriers such as the blood brain barrier and the intestinal barrier as well as general tissue edema (Vincent and De Backer 2005). Furthermore, cytokines induce activation of leukotrienes and platelet-activating factor (PAF), which have both direct effects on the endothelial surface and activate the extrinsic pathway of coagulation and production of thrombin. If the production of PAF and the potent inhibitor of fibrinolysis are active, then thrombin production results in fibrin clots. Finally, this results in the occlusion of capillaries by microthrombi and

disseminated intravascular coagulation (DIC) occurs (Bolton, Young et al. 1993; Vervloet, Thijs et al. 1998).

It is the complex microcirculatory processes of cytokine release, mediator cascades and the subsequent induction of a pro-coagulant state that leads to hypotension, inadequate organ perfusion, and necrotic cell death, all of which are associated with MODS (Multiple Organ Dysfunction Syndrome) (Lehr et al. 2000; Müller-Werdan et al. 2005).

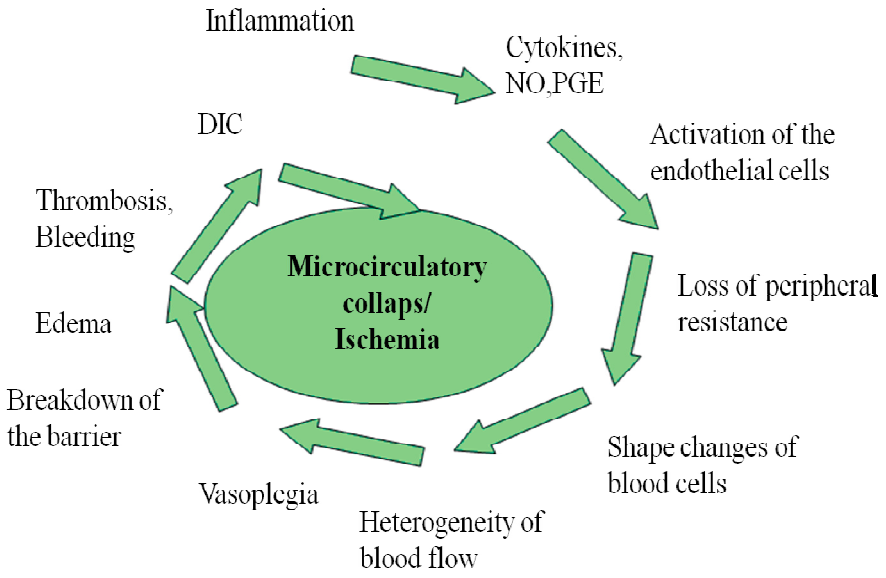

Figure 3. Motor of sepsis (Modified from Spronk, Zandstra et al. 2004)

1.1.3.1.4. General aspects of hypoxia marker during systemic inflammation

Defects in distributing blood to either the regional vascular beds or the microcirculation could be responsible for tissue hypoxia, low glucose levels, as well as high concentrations of lactate and reductive metabolites. Cells of the innate immune system must respond to these demanding conditions to maintain viability and activity. Sensing and coordinating responses to hypoxia is primarily facilitated by the transcription factor hypoxia-inducible factor (HIF). HIF-1α and HIF-2α are key regulators of the adaptive response to low oxygen under non-inflammatory conditions. Their role in a variety of pathophysiological contexts is complex and incompletely described. Despite their sequence homology, HIF-1α and HIF-2α have non-overlapping and sometimes even

opposing roles (Imtiyaz, Williams et al. 2010). Th_1 and Th_2 cytokines could affect HIF-1α and HIF-2α protein levels by regulating their transcript levels. For example HIF-2α is expressed exclusively in M_2-polarized macrophages in contrast to HIF-1α expression in M_1 macrophages (Takeda, O'Dea et al. 2010). Under septic conditions, HIF-1α and HIF-2α are differently regulated. There is evidence that HIF-1α controls inflammatory response through its regulation of the metabolic switch to glycolysis, a switch that is intrinsic to myeloid cell survival and function. HIF-1α is presented as a potential target for modulation of inflammation independent from normoxic or hypoxic environments. In contrast, HIF-2α is expressed in a more tissue-restricted manner and is not affected by LPS in normoxic tissue, but is reduced by additional inflammatory conditions (Takeda, O'Dea et al. 2010). HIF-2α serves as a conservative marker and is more relevant for hypoxia under inflammatory conditions.

1.1.3.1.5. General aspects of apoptotic marker during systemic inflammation

There are two ways by which a cell dies: by damage to the cell membrane which leads to necrosis or by apoptosis; or programmed cell death, which leads to shrinking and blebbing of the intact cell membrane. For example cell disintegration or necrosis can occur when the microvasculature is disrupted by fibrin deposition and intravascular coagulopathies. By apoptosis cells are eliminated via a programmed pathway during morphogenesis, tissue remodeling, and the resolution of the immune response. DNA fragmentation, condensation of chromatin, membrane blebbing, cell shrinkage, and disassembly into membrane-enclosed vesicles are performed in cells undergoing apoptosis. Inducers of apoptosis include steroids, cytokines such as TNF-α, IL-6, heat shock, oxygen free radicals, NO and FasL-expressing cytotoxic T lymphocytes. Apoptotic cell death occurs primarily through three different pathways: the extrinsic death receptor pathway, intrinsic (mitochondrial) pathway and the endoplasmic reticulum (ER) or stress-induced pathway. Disorganisation of apoptotic cell death might play important role in the tissue injury during sepsis. BAX promotes apoptosis and belongs to the BCL-2 family which is involved in a variety of cell processes such as controlling the release of apoptosis-inducing factor from mitochondria during apoptosis. It is suggested that BAX targets organelle membranes, including mitochondria, interacts with many anti-apoptotic factors, and is involved in apoptosis induction by directly releasing cytochrome C (Oberholzer, Oberholzer et al. 2001).

1.1.3.2. Cerebral aspects

1.1.3.2.1. Cerebral aspects of sepsis

Sepsis-associated delirium (SAD) is the new term for "septic encephalopathy", which was described in the diagnostic manual (Diagnostic and Statistical Manual (DSM-IV) and International Classification of Diseases (ICD 10). It is indicated as a severe global cerebral dysfunction. SAD is associated with endothelial activation, vascular damage, reduced cerebral blood flow, oxygen extraction by the brain, and disruption of the blood brain barrier, all of which may arise from the action of inflammatory mediators on the cerebrovascular endothelium, cerebral edema, brain inflammation and apoptosis. It results not only in nerve cell dysfunction, but also in a dysregulation of the microcirculation (Papadopoulos, Davies et al. 2000; Ebersoldt, Sharshar et al. 2007).
The brain is very sensitive to insufficient blood supply as it does not contain sufficient oxygen and substrate storage. Its energy supply is dependent on aerobic glycolysis. A few seconds of decreased oxygen leads to cellular dysfunction. There are two effective mechanisms of the brain, which maintain its adequate cerebral blood supply: neurovascular coupling and cerebral autoregulation. Under physiological conditions the activation of nerve cells induces changes in local cerebral blood flow. The neurovascular coupling mechanism adapts the brains blood circulation in accordance with local brain activity. Cerebral autoregulation compensates for systemic blood pressure changes to maintain constant cerebral perfusion. Both mechanisms are based on a complex interplay of various mediator systems. Increased NO concentration during sepsis can negatively interfere with the vasoregulative mechanisms of the brain. However, cerebral autoregulation attenuates sepsis related changes more robustly than the neurovascular coupling mechanism (Rosengarten, Hecht et al. 2008).

1.1.3.2.2. Neurovascular coupling mechanism

Various cellular processes of neurons require energy in the form of adenosine triphosphate (ATP). ATP is synthesized first by glycolysis, which is an anaerobic process and then by oxidative glucose metabolism, which requires oxygen and produces a large amount of ATP. In the brain, about 90% of glucose is metabolized aerobically. Cerebral metabolism thus depends on a constant supply of both glucose and oxygen. A continuous supply of these two energy substrates is maintained by cerebral blood flow

(CBF), which delivers glucose and oxygen to neural tissue through a complex of blood vessels. The brain is very sensitive to changes in oxygen and substrate supply, and even small perfusion variations can result in damage of brain cells. Therefore, it is important that neurons are able to balance these changes as soon as possible.

Neuronal activity induces localized changes in blood flow. There is a close relationship between neuronal activity and CBF, via the neurovascular coupling mechanism. This mechanism assures that the blood supply to the brain matches with the energy needs of the cells (Freeman 2008). Increased neuronal activity leads to release of intracellular potassium into the extracellular space resulting in activation of potassium channels, which causes dilation of the cerebral resistance vessels. This response is called "feedforward mechanism" of CBF control (Kuschinsky, Wahl et al. 1972; Kuschinsky 1991; Rosengarten, Lutz et al. 2003). After that, the reestablishment of the original extra-/intracellular distribution of ions takes place. Activation of the pumps is induced by carrying the potassium back into the cell which results in increased metabolic activity and vasodilatation. Next, the release of hydrogen ions and adenosine occurs, as long as a mismatch between oxygen/glucose demand and CBF supply exists. CBF is higher while counteracting this mismatch. This results in a so-called "feedback mechanism". However flow regulation is a complex process which involves mediators such as adenosine, NO and others.

LDF (Laser-Doppler-Flowmetry) is a vascular-based brain imaging technique that infers local changes in the dynamic vasoregulative functions of the activation flow coupling. It has been widely used to study evoked flow response in the cerebral cortex during somatosensory stimulation. This technique measures flow velocity rather than flow, but the relative signal changes allow accurate analysis of regional blood flow. The LDF signal is proportional to the number of red blood cells moving in the measuring volume multiplied by the mean velocity of these cells, respectively representing blood cell flux. In this study, neurovascular coupling measurements were performed with electrodes attached to the right forepaw and to the LDF (Dirnagl, Kaplan et al. 1989; Rosengarten, Lutz et al. 2003).

1.1.3.2.3. Somatosensory evoked potentials

Evoked potentials are the electrical signals generated by the nervous system in response to sensory stimuli. Somatosensory evoked potentials (SEP) consists of a series of waves that reflect sequential activation of peripheral nerves along the somatosensory pathways and induced cortical response. After stimulation of the nerve it comes to an electrical discharge (depolarization) of the cell, which generates an electrical impulse called an action potential. Brain electrical activity is recorded by a computer which analyzes the speed, duration, and intensity of the neural response as well as an amplifier, filter and computer averaging software for better representation of the data.
SEP is known to be a sensitive parameter for early diagnosis of SAD in intensive medical care units. Even if the first neurological abnormalities failed, SEP provides sensitive index of brain dysfunction. It shows general alterations which increase parallel to the severity of the systemic inflammatory process. In this study, SEP and latencies are performed using Electroencephalography (EEG)-recording (Ohnesorge, Bischoff et al. 2003; Rosengarten, Hecht et al. 2007).

1.2. Aim of the study

Endotoxin animal models are mainly used to analyze the complexity of the circulatory and metabolic alterations involved in sepsis in the entire organism. Moreover it is important to develop a reproducible and satisfactory small animal sepsis model which simulates sepsis associated organ dysfunction. However *in vitro* experiments cannot reproduce the systemic inflammatory process entirely, but can make an important contribution in regards to the understanding of the function of different agents. Sepsis induction in endotoxin animal models can be performed by intravenous, intraperitoneal, or intratracheal administration of toxins (LPS) or live bacteria, which results in bacteremia. Administration of endotoxin or performance of cecal ligation and puncture (CLP) causes an overwhelming innate immune response, which has some similarities to human sepsis. In this study, sepsis was induced in rats by intravenous administration of 5 mg/kg LPS, as this model is standardized and induces sepsis quickly (Dyson and Singer 2009).

Microcirculation may play a key role in the pathogenesis of sepsis-related organ dysfunction, especially in the first 6 to 24 hours after infection. Even though have been intensive studies in this field, the complexity of the sepsis mechanism still remains poorly understood and needs further investigations. Increased TNF-α production has been shown to be critical for the initiation of the pro-inflammatory response. Preclinical studies with antibodies against TNF-α have shown good effects in experimental models when the drugs are administered before the inflammatory challenge, but the end result of the inflammation response did not change (Minnich and Moldawer 2004). Another potential candidate for diagnosis and therapy of early sepsis was protein C as decreased levels were associated with an increase in mortality by patients. Limited analysis in humans showed that administration of activated protein C or protein C resulted in reversed haemostatic alterations and organ dysfunction in septic patients (Fisher and Yan 2000).

Less clear are the mechanisms resulting in microcirculatory failure in the brain under septic conditions. In previous studies, it was shown that measurements of SEP and latencies via EEG as well as neurovascular coupling and resting flow velocity recording via LDF, could be used as early prognostic indicators of systemic inflammatory response. Changes in SEP are sensitive markers for diagnosis of SAD and sepsis. It was shown that SEP amplitudes and related evoked flow velocity responses of the neurovascular coupling dropped when macrocirculation was still intact (Rosengarten, Hecht et al. 2007). MRI-technique was used as a sensitive parameter for detection of early microcirculatory brain dysfunction, but there was no detection of subtle brain edema 3.5 hours after sepsis induction. Furthermore, neurovascular coupling mechanism and somatosensory evoked potentials are more reliable for detection of early cerebral dysfunction (Zauner, Gendo et al. 2002; Ohnesorge, Bischoff et al. 2003; Rosengarten, Walberer et al. 2008).

Other studies were focused on iNOS inhibition as a possible therapy in the modulation of the inflammatory response. iNOS inhibitors like 1400W did not affect the immune response or prevent microcirculatory collapse, and also the effects on sepsis outcome were mostly negative by patients. That is the reason why iNOS-inhibition can not be recommended for clinical practice (Vromen, Arkovitz et al. 1996; Wray, Millar et al. 1998; Lee, Lin et al. 2005).

An ideal agent to recruit the microcirculation during sepsis would most likely be the stimulation of the vagus nerve. Some researchers have tried to define the mechanism of

efferent vagal signaling on the inflammatory response. These investigators supposed that acetylcholine binds to the α7 nicotinic cholinergic receptors expressed by macrophages and other cell types and reduced the release of pro-inflammatory cytokines such as TNF-α in rats (Borovikova, Ivanova et al. 2000; Tracey 2002). It was shown that electrical vagus nerve stimulation inhibited the acute inflammatory response to acute hypovolemic hemorrhagic shock (Guarini, Altavilla et al. 2003), splanchnic artery occlusion shock (Altavilla, Guarini et al. 2006) and intestinal inflammation during experimentally induced ileus (de Jonge, van der Zanden et al. 2005). It also diminished shock and reduced pro-inflammatory cytokines synthesis in the livers and hearts, obtained from animals subjected to ischemia-reperfusion injury induced by transient aortic occlusion (Bernik, Friedman et al. 2002), as well as reduced localized inflammation in the murine arthritis model (Borovikova, Ivanova et al. 2000). This concept of vagal inflammatory reflex was followed by many other studies, but there is still no exact explanation about how vagus nerve stimulation affects sepsis.

New therapeutic approaches which counteract microcirculatory failure could represent a novel strategy to help optimize the inflammatory response. The impact of sepsis on brain microcirculation is not well defined. Using a reproducible animal model of septic shock, this study sought to investigate whether vagus nerve stimulation protects the cerebral microcirculation and neuronal functions as well as its connection to NO signalling. The working hypothesis of this study suggests that vagus nerve stimulation during septic shock may attenuate the hyper-inflammatory host response and result in lower iNOS-levels. We proposed that vagus nerve stimulation during sepsis would decrease the severity of microcirculatory failure in the brain, which is an early prognostic parameter of sepsis outcome. Neurovascular coupling via LDF and SEP are measured in rodents and collect to clinically relevant data. Investigations of the effects of vagus nerve stimulation on released pro- and anti- inflammatory cytokines, NO-, hypoxia– and apoptosis signalling in endotoxinemic rats were performed and analyzed.

2. MATERIALS AND METHODS

2.1. Laboratory animals

Adult male Sprague Dawley rats (290-320 g) were purchased from Harlan Laboratories (Harlan, Rossdorf, Germany). They were housed five to a cage with food and water available *ad libitum* and were maintained on a 12-hour light/dark cycle (lights on at 7 a.m.). All procedures performed on the animals were in strict accordance with the National Institutes of Health Guide for Care and Use of Laboratory Animals and approved by the local Animal Care and Use Committee. The Institutional Review Board for the care of animal subjects approved the study.

2.2. General preparation

2.2.1. Overview of the experimental station

The arrangement of the experimental instruments is shown in Figure. 4. Instruments are labeled accordingly.

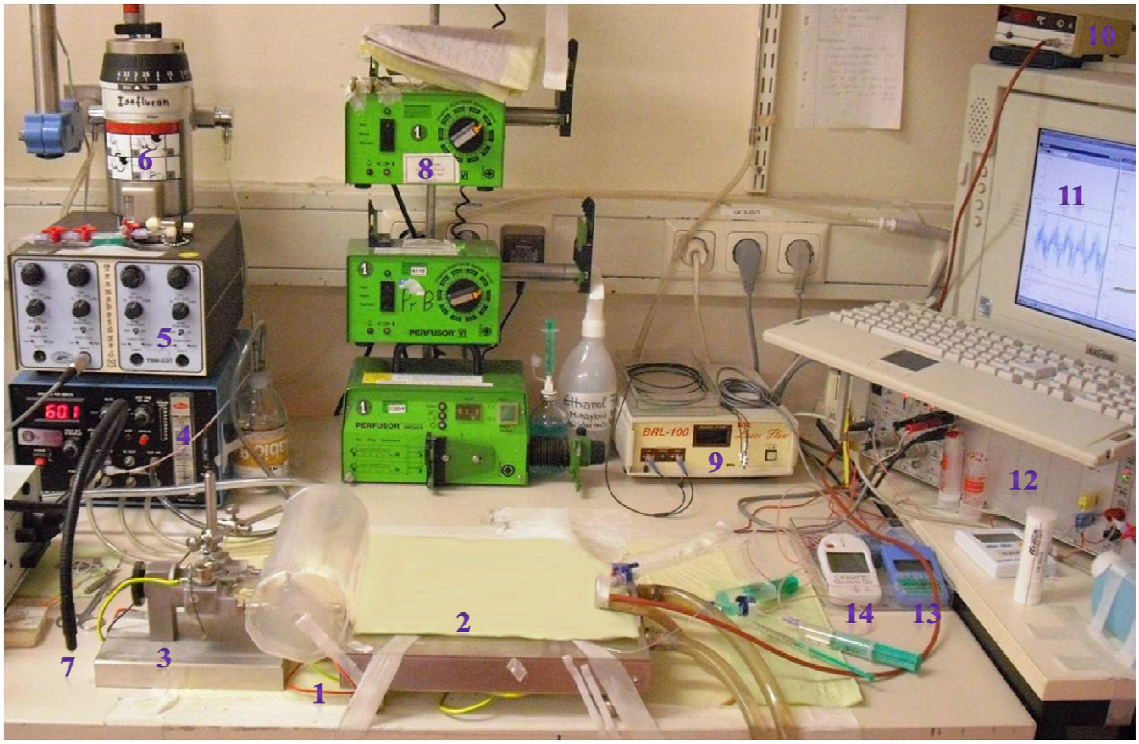

Figure 4. Experimental Instrumentation: 1. Stimulation needles, 2. Heating pad, 3. Stereotaxic frame, 4. Ventilator pump, 5. Amplifier 1, 6. Isofluran pump, 7. Light source, 8. Perfusor, 9. LDF, 10. Thermometer, 11. PC with Neurodyn Software, 12. Amplifier 2, 13. Lactate indicator, 14. Glucose indicator

2.2.2. Inhalatory anesthesia

Rats were initially anesthetized in an isoflurane saturated box until they achieved the tolerance phase III of anesthesia (1-2 minutes). After that they were brought in a supine position over the heating pad. The head of the rat was placed into a breathing mask, which was connected to isoflurane ventilator system. The animals were consistently anesthetized with 1.5 to 3% of isoflurane in 1:1 nitrous oxide (N_2O)/(O_2) oxygen mixture, through the breathing mask. This inhalation was adapted individually according to the animal's constitution. After they achieved tolerance phase III, the interdigital reflex was checked and the surgical intervention started. Rectal body temperature was recorded continuously and maintained at 37°C using a feedback-controlled heating pad.

2.2.3. Cannulation of artery and vein femoralis

The hindlimbs of the animal were fixed on the heating pad with tape. After disinfection of the surgical location, 1.0-1.5 cm skin incision was made in the medial inner shank to expose the abdominal muscles. The tissues were moved aside to reveal A.femoralis, V.femoralis, and N.femoralis, using a wound spreader.

The vessels were dissected from the surrounding tissues using anatomic iris forceps. The distal part of the vessels was closed with a ligature. Cannulation was achieved from two opened ligatures: the first open ligature was placed around the proximal portions of the femoral artery; the second open ligature was placed around the proximal portions of the femoral vein. To avoid thrombosis, the catheter was filled with heparin overnight and flushed with saline solution just before the cannulation.

Cannulation was performed first on the artery and than on the femoral vein. An Aesculap clip was placed just above the prepared open ligature so that the blood supply was interrupted in the cannulated field for a short time. The vessel cut was done using the scissor “Nachstar from Vannas” and the catheter was inserted into it, just under the clip. After the clip was removed, the catheter was advanced to its final position and fixed with the prepared proximal ligature. Cannulation of the femoral vein was performed similarly, by which the catheter was advanced up towards the V.cava inferior. To fix both catheters, a massive ligature was placed over the other ligatures, followed by tape fixation at the Achilles tendon.

2.2.4. Tracheotomy and intubation

After cannulation the rat was prepared for tracheotomy under the following procedures: the neck area was disinfected with ethyl alcohol, followed by a cutaneous incision starting 1 to 2 cm from the breast bone extending to the mid-cranial neck, was performed to expose the neck muscle and salivary glands. Next, the neck muscles were dissected carefully in their medial part and kept apart with wound retractor. A preparation was done around the trachea with anatomical iris forceps in layers until it lay bare. An opened ligature was placed around the trachea for later fixation of the tracheal tube. Just before the start of the tracheotomy, anesthesia with isoflurane was reduced to 1% to prevent possible overdoses of anesthetics. The trachea was cut between the fourth and fifth cartilage rings, the trachea tube was inserted and fixed together with the trachea through the ligature. The breathing mask was removed. The trachea tube was connected immediately to the ventilator system. This moderation was done quickly without the animal waking up.

After tracheotomy and intubation the respiratory rate was maintained at 60 breaths per minute, an inspiration time at 0.75 seconds, and the respiratory pressure volume at 700 cc per minute by PEEP (positive end-expiratory pressure) of 4 cm of water column during the entire experiment.

2.2.5. Injection anesthesia and muscle relaxation

After intubation, isoflurane narcosis was discontinued and replaced by an intravenous application of α-chloralose/borax–anesthesia, which was administered through the femoral catheter set. First a stock solution of α-chloralose and borax was prepared as follows: 350 mg Borax and 250 mg of α-chloralose were dissolved in 10 ml 0.9% sodium chloride (NaCl-solution) warmed at 40°C using a magnetic stirrer bar until the solution was free from borax crystals. In addition this mixture was filtered in 3 ml syringe using a Millipore filter (Millex ® GP filter) and injected intravenously in the following dose: an initial dose at 60 mg/kg body weight, washout period of 60 minutes for each animal, followed by a supplementary dose at 30 mg/kg body weight every hour.

The spontaneous breathing of the animals was paralyzed by an additional intravenous administration of 0.3 ml pancuronium bromide initially. Supplementary dosage of this muscle relaxant was given via perfusor syringe pump, whereas it was diluted in 0.9%

NaCl 1:10 and given 1.2 ml per hour. This infusion was used also as a volume compensatory therapy. During α-chloralose anesthesia, the animals were ventilated with a 1:1 mixture of nitrogen and oxygen.

2.3. Preparation and stimulation of vagus nerve

The vagus nerve of each side was exposed lateral of the trachea running in parallel with the common carotid artery in the cervical area. The right nerve was carefully dissected from the artery in each rat using the fine iris forceps, while the left nerve was used for the experiments. This preparation was done precisely without any damage of the nerve fibres. Whereas the nerves were kept intact in the control group (SHAM), both nerves were dissected in the vagotomy group (VGX). In the group with vagus nerve stimulation both vagus nerves were dissected and the left distal part of the nerve was secured in a special nerve stimulation clamp to allow electrical stimulation (VGX+STIM). Electrical pulses were applied with 2 mA, 0.3 ms pulse width, and 2 Hz repetition frequency and stimulation was performed for 10 min. Stimulation blocks were repeated every 45 min, starting before the application of endotoxin and continuing until the end of experimentation. In the groups without stimulation, no special treatments were undertaken during these 10 minutes.

2.4. Preparation for neurovascular coupling and data valuation

2.4.1. Preparation for neurovascular coupling

After the preparation of the vagus nerve, the rat was turned over onto its abdomen. The head was fixed in a stereotaxic frame with bolts in the ear canal. In this case it is important not to cause a perforation of the tympanic membrane, because this could cause pain and disturbe the experimental measurements (Figure 5). The upper incisors were hitched on the frame. Afterwards the skin over the parietal bone was cut at approximately 1 cm from where a tunnel under the skin and above the nasal bone was prepared using the “Metzenbaum” scissor. An electrode was inserted subcutaneously into the tunnel up to the nose to neutralize the other electrode over the cortex. The voltage differences between the electrodes were used for measurements of the EEG and the resulting SEPs.

The tissues above the left parietal bones and the connecting periosteum were removed using a “Nachstar” scissor and an anatomical iris forceps so that the apex of the skull was exposed. The bleeding from the small vessels was interrupted by electrocauterization. Using a microscope, the left parietal cortex was thinned with a saline-cooled drill up to the layer of compacta interna until an area was reached where the blood vessels appeared. No damage occurred to the underlying dura mater or the brain. This preparation allowed transcranial LDF.

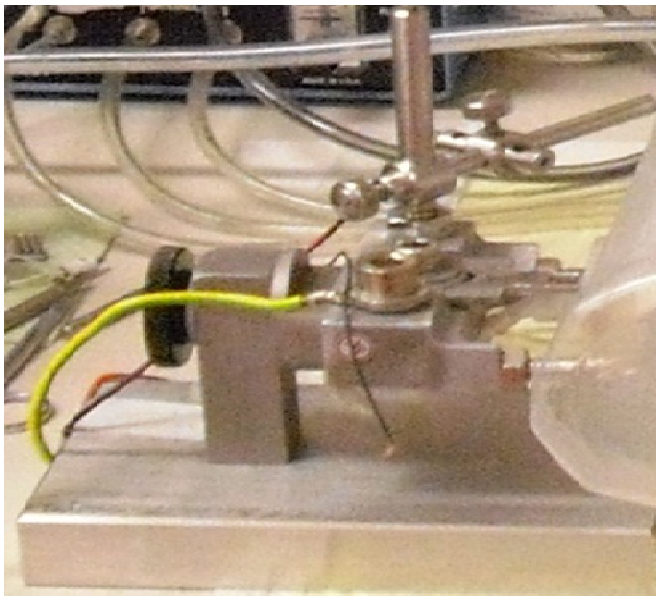

Figure 5. Overview of the stereotactic frame

The apex of the skull was exposed, and the bone over the left parietal cortex was thinned with a saline-cooled drill to allow transcranial LDF. The laser probe was placed on the thinned skull 3.5 mm lateral and 1 mm rostral to the bregma in accordance with the coordinates of the somatosensory cortex; a location that corresponds closely to the region of maximal hemodynamic response during contralateral forepaw stimulation. The meaning "bregma" comes from the craniometry. It describes the point at which the sutura coronalis (which separates the frontal from the parietal bone) and the sutura sagittalis (which separates the two parietal bones) meet each other. The laser-Doppler signal was found by 300-350 Flux blood cell velocity, which responds to the capillary field.

Brain electrical activity was recorded monopolarily with an active silver chloride electrode placed 0.5 mm behind the laser probe and with an indifferent calomel electrode placed on the nasal bone. Somatosensory stimulation was achieved with

electrical pulses applied by small needle electrodes inserted under the skin of the right forepaw. The pulses consisted of rectangular bipolar pulses of 1.5 mA and a pulse width of 0.3 ms. The pulse repetition frequency was set at 2 Hz and stimulations were carried out for 30 s. Stimulation with 1.5 mA ensured the pain fibres were unaffected and thereby prevented changes in blood pressure. A rest of 30 s following each stimulation period was performed while activation rest cycles were repeated 10 times to increase signal to noise ratio (Figure 6). In addition, the grounding of the stereotactic frame and the NaCl electrode was connected to the computer for analysis.

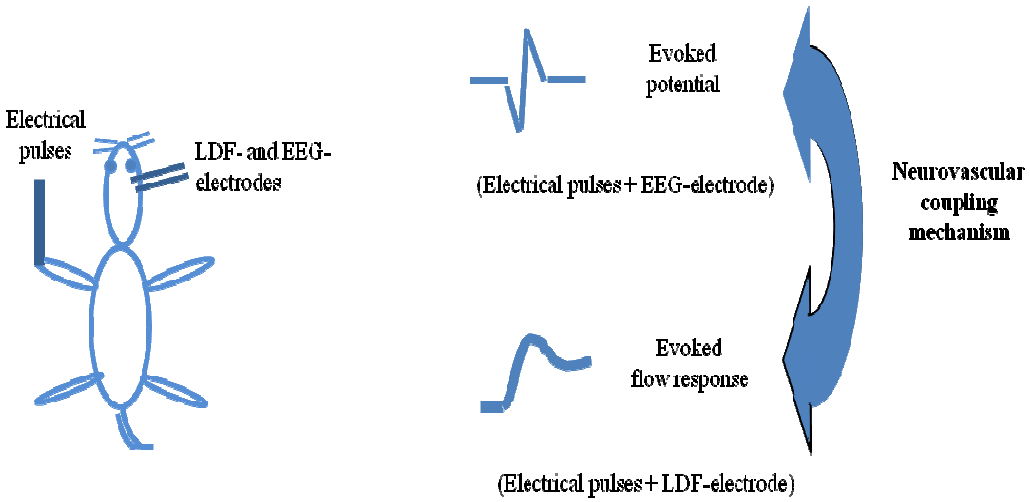

Figure 6. Experimental design for measurements of the neurovascular coupling.

The head of the rat was turned 45° to the right with the rotating stereotactic frame and its body position was moved to the right about 90°. Before the electrodes were placed around the nerve, the cervical area was expanded using a wound retractor from "Logan modell Reill" for better overview. To prevent possible damage of the artery communis and the surrounding tissues, two cotton particles were set between the artery and the vagal nerve. The whole preparation took approximately 1 hour.

Experimental preparation and procedures are shown schematically on Figure 7.

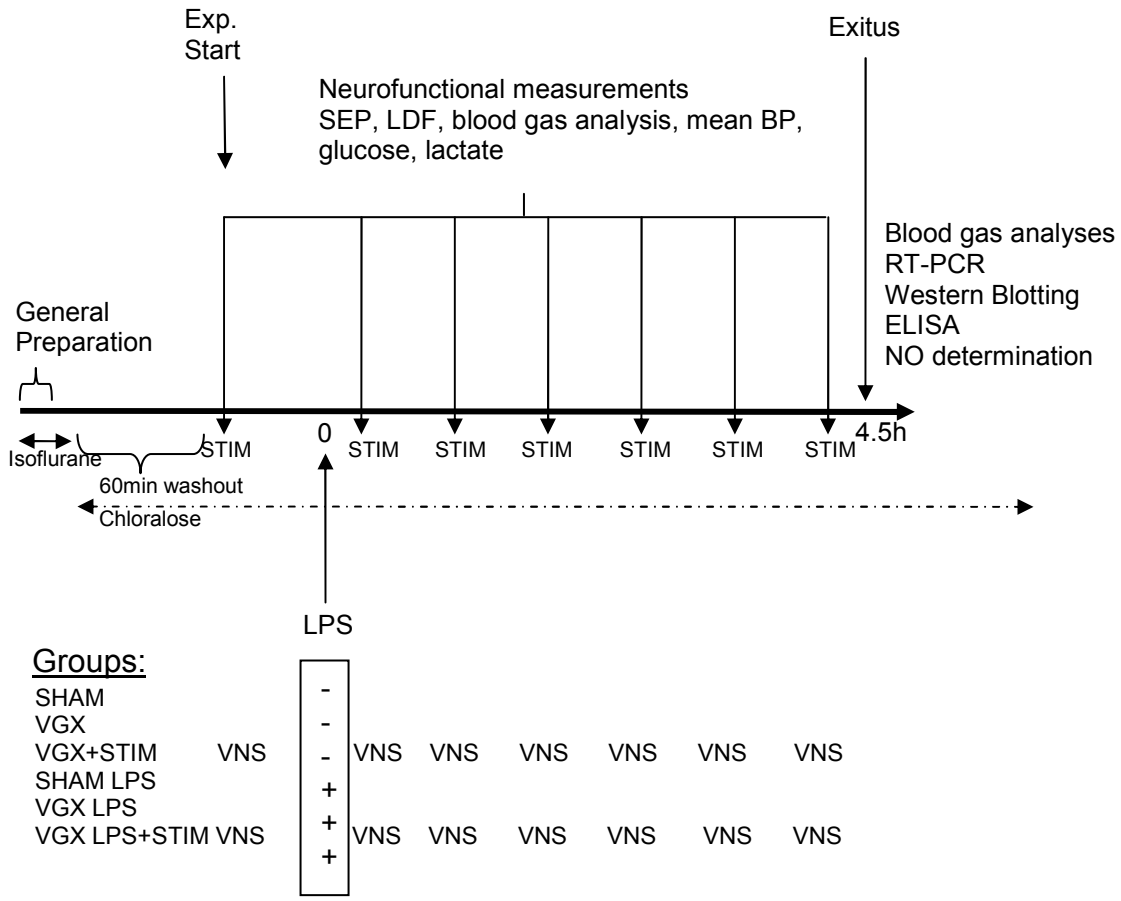

Figure 7. Illustration of the preparation period and experimental protocol together with time points of vagal interaction or neurofunctional measurements.

2.4.2. Data evaluation

Evoked potential amplitudes were calculated from the N1-P1-amplitude differences and the latency between the beginning of stimulation and the occurrence of the P1-peak was examined. SEPs were averaged and the resulting convolutions were described as follows: upward amplitudes were defined as “negative” and downward amplitudes as “positive”. The “positive“ peaks were marked as “P” and the “negative” peaks as “N”. The recording of evoked potentials on the head starts with a positive peak (P1), followed by a negative one (N1) and again a positive peak (P2) (Figure 8).

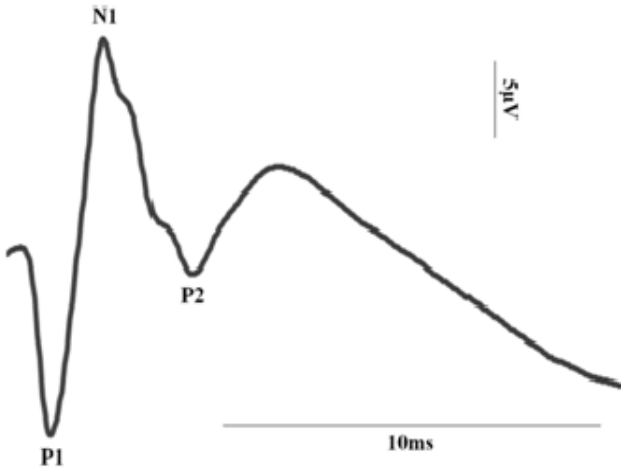

Figure 8. SEP during stimulation of the contra lateral forepaw. 60 signals were averaged throughout 30 s stimulation.

The evoked flow velocity responses were calculated from the averaged relative flow velocity signals under conditions of stimulation. Figure 9 presents flow response data of 10 stimulation cycles as well as a comparison between the increase of blood flow during stimulation and the resting flow. Rodents were electrically stimulated for 30s and rested for 30s for a period of 10 minutes. The measurements were averaged. Signals were recorded and amplified and SEPs were averaged using the Neurodyn acquisition software.

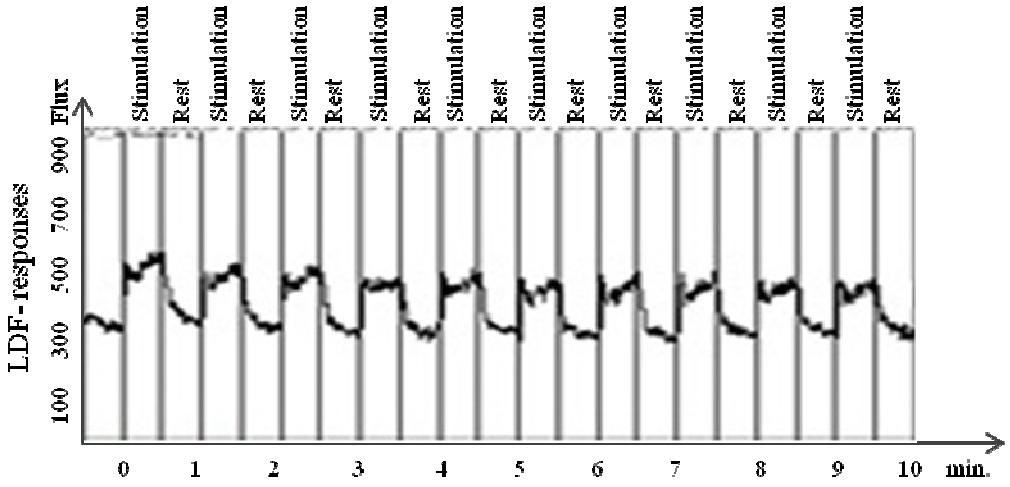

Figure 9. LDF response of somatosensory cortex area during contra lateral forepaw stimulation. One stimulation cycle involved 30 s stimulation and 30 s at rest. 10 cycles are shown.

2.5. Study design

In random order, 60 rats received intravenously 5 mg/kg body weight LPS or 0.5 ml of 0.9% NaCl. LPS was dissolved in 0.5 ml of 0.9% NaCl and slowly administered within 5 min intravenously. Endotoxinemic and sham groups were further divided into three subgroups each. In one subgroup, bilateral vagotomy (VGX) was performed without stimulation of the vagal nerve (LPS group: VGX LPS; non-septic group: VGX). In a second group, the distal part of the left vagus nerve was stimulated (LPS group: VGX LPS+ STIM; sham group: VGX+ STIM). In a third group, the operation of the vagus nerve was stopped before vagotomy (LPS group: SHAM LPS; non-septic group: SHAM). Each experimental group consisted of 10 animals. Experiments were performed up to 4.5 h after LPS/vehicle administration.

Blood samples were obtained directly from the left ventricle of the heart before the rats were killed. Afterwards a heart perfusion was performed with saline so most blood was removed from the brain vessels for precise analyzes. For this procedure, the rat was laid on its back, the cranial abdominal cavity cut 3 cm distal from the xiphoid process and lateral parallel to the costal arch using a scissors to expose the diaphragm. With next incision the diaphragm which was separated from the costal arch, followed by 3-4 cm incisions parallel to the sternum. The costal arch was moved aside and fixed by two clamps to the left and to the right. The apex of the heart was fixed by forceps and 1 ml blood was taken direct from the left ventricle. The vena cava ending into the right atrium was truncated in order to drain the liquid during perfusion. A perfusion tube was inserted into the left ventricle and saline was flushed through the systemic circulation and drained from the truncated vena cava. After perfusion 1 ml KCl was injected intravenously. The brain was removed rapidly and stored at -80°C.

2.6. Laboratory analysis

2.6.1. Blood parameters

The ventilation of the animals was controlled continuously throughout the entire experiment. The measurements of arterial blood pressure, body temperature, glucose and lactate as well as the blood gas parameters were also recorded continuously. The glucose and lactate parameters as well as the following blood gas parameters: pH, pO_2, pCO_2 and hemoglobin were determined from arterial blood samples using blood gas analyzer.

The blood samples were taken from the arterial catheter using hematocrit capillary tubes. For this procedure the arterial catheter was disconnected by a scissor clamp, the pressure transducer was removed, and the scissor clamp was opened cautiously so that a drop of blood could form at the end of catheter. Sticks from glucose and lactate sets were placed to the blood drop as well as the hematocrit capillary tube so that they filled with blood. Next, the artery catheter was flushed with saline to prevent possible formation of blood clots and the pressure transducer was connected to it. The hematocrit capillary tube was inserted into the blood gas analyzer for measurements. Within a minute, results of the glucose and lactate set were obtained.

2.6.2. Polymerase chain reaction (PCR)

2.6.2.1. RNA isolation

Total RNA from tissue was extracted using Trizol according to the manufacturer's instructions. 100 mg brain tissue was applied to 1 ml Trizol and homogenized by Precellys24 homogenizer. Trizol lysates were kept at room temperature (RT) for 10 min to dissociate the RNA from histone proteins. Then 0.2 ml of chloroform was added, vigorously mixed for 15 sec and centrifuged at 10500 rpm for 15 minutes at 4°C. After that, the transparent upper layer was carefully transferred to a new tube and gently mixed with 0.5 ml Isopropanol. After 10 min the mixture was centrifuged at 10500 rpm for 10 minutes at 4°C and the RNA pellet was washed with 1 ml 75% ethanol and air dried. RNA was dissolved in DEPC-water and stored at -80°C. The concentration and quality of RNA were estimated by NanoDrop spectrophotometer.

2.6.2.2. Reverse transcription-PCR (RT-PCR)

cDNA was synthesized by a two-step RT-PCR using ImProm-II™ reverse transcription system according to the manufacturer's instructions. 8 µg RNA and 2 µl Oligo(dT)15-Primer were incubated at 70°C for 6 min, followed by a quick chill at room temperature for 5 min and addition of 30 µl reaction B. The reverse transcription reactions were subjected to cDNA synthesis by annealing at 25°C for 5 min and incubating at 42°C for 60 min, followed by thermal inactivation of reverse transcriptase at 70°C for 15 min. The cDNA was stored at -20°C.

Reaction A component	Volume	Final concentration
RNA, [0.1 µg/µl]	8 µl	0.8 µg
Oligo(dT)15- Primer [500 µg/ml]	2 µl	25 ng

Reaction B component	Volume	Final concentration
ImProm-II™ 5X Reaction buffer	8 µl	1 X
MgCl2, 25 mM	4 µl	2.5 mM
dNTP mix, [10 mM]	2 µl	0.5 mM
RNasin® ribonuclease inhibitor	1 µl	1 U/µl
ImProm-II™ reverse transcriptase	2 µl	
DEPC-water	13µl	

2.6.2.3. Quantitative real time-PCR (qRT-PCR)

Intron-spanning primer pairs were designed using the Primer 3 program and are shown below. Primers were cross-checked to insure the specificity by blasting to the whole genome. The product size is controlled within the range of 80 bp-150 bp.

qRT-PCR reaction component	Volume	Final concentration
cDNA 0.25µg/µl	2 µl	0.5 µg
MgCl2, 50 mM	1 µl	5 mM
ROX, 25 µM	0.1 µl	0.1 µM
Upstream primer, 10 µM	0.5 µl	0.2 µM
Downstream primer, 10 µM	0.5 µl	0.2 µM
Platinum ®SYBR® GreenER™ SuperMix		
Universal buffer	12.5 µl	1 X
DEPC-water	8.4 µl	

qRT-PCR was performed on a Mx3000P® QPCR system machine using SYBR® GreenER™ qPCR SuperMixes Universal kits according to manufacturer's instructions. For the negative control, cDNA was omitted. The annealing temperature for every gene was 58°C. By using the MxPro™ QPCR software, a dissociation curve was generated for each gene to ensure single product amplification and the threshold cycle (C_t values) for each gene was determined. The comparative $2^{-\Delta\Delta Ct}$ method was used to analyze

mRNA fold changes between SHAM and LPS-treated groups, which was calculated as Ratio = $2^{-(\Delta Ct\ control-\Delta Ct\ MCT)}$ where C_t is the cycle threshold, and ΔC_t (C_t target—C_t reference) is the C_t value normalized to the reference gene Porphobilinogen Deaminase (PBGD) obtained for the same cDNA sample. Each reaction was run in duplicate and repeated three times independently. The calculated $2^{-\Delta\Delta Ct}$ was transformed into a percentage using the control as 100% to show the mRNA expression difference.

qRT-PCR programm	**Temperature**	**Time**	**Cycle**
Activation	95°C	10 min	1
Denaturation	95°C	30 sec	40
Annealing	58°C	30 sec	40
Extension	72°C	30 sec	40
Denaturation	95°C	1 min	
Dissociation curve	55-95°C	indefinite	1
Soak	4°C	indefinite	1

Primers for qRT-PCR:

Rat porphobilinogen deaminase PBGD:

Forward 5'-CAAGGTTTTCAGCATCGCTACCA-3'

Reverse 5'-ATGTCCGGTAACGGCGGC-3'

Rat inducible nitric oxide synthase iNOS:

Forward 5'-CAGCCACCTTGGTGAGGGGA-3'

Reverse 5'- TCCAGGGGCAAGCCATGTCT-3'

Rat Bcl-2-associated X protein BAX:

Forward 5'-CAAGAAGCTGAGCGAGTGTCT -3'

Reverse 5'-CAATCATCCTCTGCAGCTCCATATT-3'

2.6.3. Western blotting

2.6.3.1. Protein isolation

Total protein was extracted in RIPA buffer containing 1x TBS, 1% Nonidet P-40, 0.5% sodium deoxycholate, 0.1% SDS, 0.004% sodium azide. PMSF, proteinase inhibitor cocktail and sodium orthovanadate (10 µl each in 1 ml RIPA) were added to RIPA

freshly before use. 100 mg brain tissue homogenized in 800 µl RIPA was centrifuged under 12000 rpm for 30 min at 4°C and the supernatants were stored at -80°C.

2.6.3.2. Protein concentration analysis

A series of bovine serum albumin (BSA) solution from 0.25-2 µg/µl were used as standard. The protein samples were pre-diluted into the range of the standard and the concentration of each sample was double estimated by D*c* protein assay kit based on the Bradford method using a microplate reader.

2.6.3.3. SDS-polyacrylamide (SDS-PAGE) gel electrophoresis

Protein samples of the same concentration were mixed with 5x SDS gel loading buffer at a ratio of 4:1 (v/v) and denatured at 100°C for 5 min. Protein samples or rainbow markers were loaded into the wells of 10% SDS-PAGE gels and ran at 100-130 V for 2-3 hours of separation. Buffers are listed as follows.

5×SDS gel-loading buffer component	**Final concentration**
Tris-Cl (2 M, pH 6.8)	375 mM
SDS	10% (w/v)
Glycerol	50% (v/v)
β-Mercaptoethanol	12.5% (v/v)
Bromophenol blue	0.02% (w/v)
Running buffer component	**Final concentration**
Tris-HCl	25 mM
Glycine	192 mM
SDS 10% (w/v)	0.1% (w/v)

Separating gel (10%) component	**Volume**	**Final concentration**
Tris-Cl (1.5 M, pH 8.9)	1.5 ml	375 mM
Acrylamid 30% (w/v)	2 ml	10% (w/v)
SDS 10% (w/v)	60 µl	0.1% (w/v)
APS 10% (w/v)	30 µl	0.05% (w/v)
TEMED	6 µl	0.1%
H_2O	2.4 ml	

Stacking gel (6%) component	Volume	Final concentration
Tris-Cl (0.5 M, pH 6.8)	625µl	125 mM
Acrylamid 30% (w/v)	500µl	10% (w/v)
SDS 10% (w/v)	25 µl	0.1% (w/v)
APS 10% (w/v)	12.5 µl	0.05% (w/v)
TEMED	2.5 µl	0.1%
H_2O	1.34 ml	

2.6.4. Measurement of NO concentration in plasma samples

NO metabolites including nitrite and nitrate were determined for the sepsis groups and for the non-LPS control group (SHAM) in n=10 plasma samples each by NOASievers 280 according to manufacturer's instructions. The principle of NO measurement depends on the reduction of nitrite and nitrate by vanadium chloride in hydrochloric acid at 95°C to NO gas which is given to the Nitric Oxide-analyzer connected to a computer for data transfer and analysis by using "NoaWin 32" software.

For this measurement the plasma samples containing high concentrations of protein were deproteinized prior to analysis via cold ethanol precipitation. Contamination from nitrite or nitrate could occur during this procedure, especially if the reagents were contaminated. For this reason a blank was included to check for contamination.

An antifoaming 204 agent; a mixture of non-silicone organic defoamers in a polyol dispersion 100 µl, was added to the vessel containing vanadium chloride solution at the beginning of the experiment. To prevent damage to the NOA from hydrochloride acid vapour, a gas bubbler filled with aqueous sodium hydroxide was installed between the purge vessel and the NOA. A standard solution of 100 mM sodium nitrite was prepared and dilutions of the standard were used for constructing the calibration curve. NO concentration was determined from the peak, which appears about 30 seconds after injection of the sample. All samples were measured in triplicates.

2.6.5. Enzyme-linked immunosorbent assay (ELISA)

Following the experiments, blood samples were drawn into tubes containing Heparin-sodium 2500 (Ratiopharm, Ulm, Germany). They were immediately centrifuged and separated, and the plasma was stored at -80°C until analysis. Concentrations of cytokines including IFN-γ, TNF-α, IL-6, IL-10 in plasma samples were determined by

ELISA kits (BD Bioscience, Heidelberg, Germany) for each LPS group (n=6) as well as for the SHAM group.

2.7. Statistic

Statistical evaluation of all data was performed with ANOVA to assess differences between the groups. In cases of significance, a Sheffè *post-hoc* test was applied. If the assumptions of normal distribution and equality of variances could not be assured in the statistic F-test, a nonparametric Paired-Sign or Kolmogorov-Smirnov test was conducted (Statview, SAS, USA). The significance level was set to $p<0.05$.

2.8. Substances and Instruments

Table 1 lists all materials used for the experimental and laboratory analysis. In Figure 10 all instruments used in the experiment are listed.

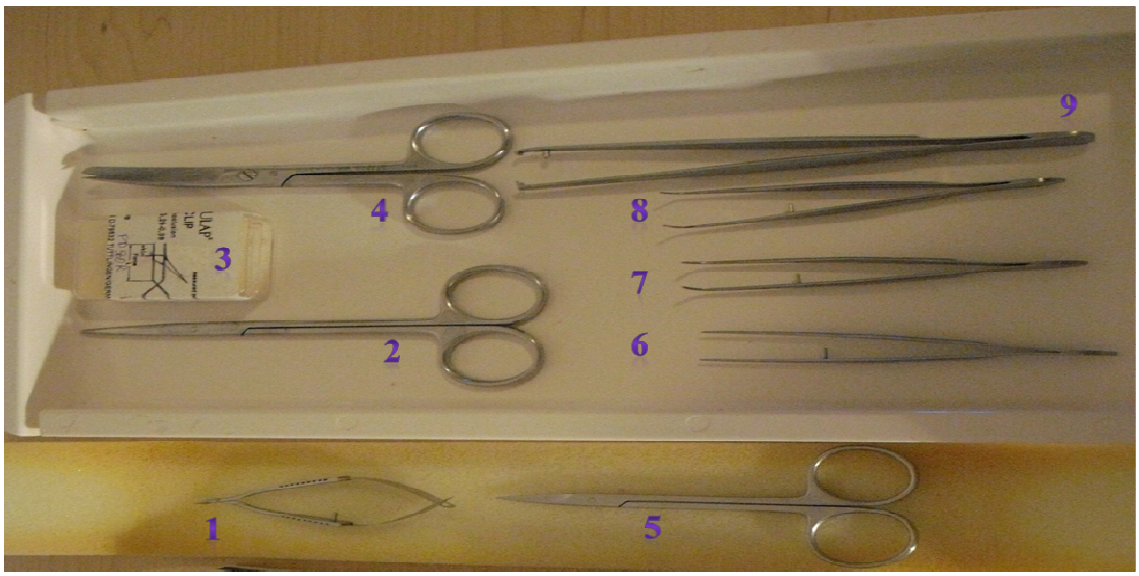

Figure 10. Instruments used for surgery interventions: 1. Nachstar scissor from Vanna; 2. Metzenbaum scissor; 3. Aesculap clip; 4. Anatomic scissor; 5. Fine scissor; 6,7,8. Anatomic iris forceps; 9. Forceps for the clip

Table1. Materials

Material	Company	Unit	Address of the company
Isofluran	Baxter	250 ml	Baxter Deutschland GmbH, 85716 Unterschleißheim
Gas mixture	Nitrogen 5.0, Oxigen 5.0	100 l	Air Liquide
Isotone NaCl	DeltaSelect GmbH	100 ml	DeltaSelect GmbH 72793 Pfullingen
Kaliumchlorid 7,45% (coloured)	BiBraun Melsungen AG	100 ml	B.Braun Melsungen AG 34209 Melsungen
Heparin-Natrium 2500	Ratiopharm	5x5 ml	Ratiopharm GmbH 89070 Ulm
Chloralose,α-Chloralose	Sigma-Aldrich	100 g	Sigma -Aldrich Chemie GmbH 89555 Steinheim
Borax,Natriumtetraborate 99%	Sigma-Aldrich	100 g	Sigma -Aldrich Chemie GmbH 89555 Steinheim
Pancuronium Inresa,Pancuroniumbromid	Inresa	10x2 ml	Inresa GmbH 79114 Freiburg
Lipopolysaccharid E.coli, O111:B4, L2630, LOT 115K4092	Sigma-Aldrich	400 mg	Sigma -Aldrich Chemie 82024 Taufkirchen
Trachea tube	BD Microlance	shorted to 1.5 cm	Becton Dickinson,Germany
Arterenol®1ml Norepinephrinhydro chlorid	Aventis	1 ml	Aventis Pharma Deutschland GmbH 65926 Frankfurt am Main
Softasept®N	BiBraun Melsungen AG	250 ml	B.Braun Melsungen AG 34209 Melsungen
Haematokrit -capillary Na-Heparin	Hirschmann Laborgeräte	10x100 articles	Hirschmann Laborgeräte GmbH&Co.Kg 74246 Eberstadt
Syringe Inject-F	BiBraun Melsungen AG	1 ml, 2 ml, 4 ml, 10 ml, 20 ml	B.Braun Melsungen AG 34209 Melsungen
Original -Perfusor® Syringe OPS	BiBraun Melsungen AG	50 ml	B.Braun Melsungen AG 34209 Melsungen
Original -Perfusor® Charge OPS	BiBraun Melsungen AG	150 cm	B.Braun Melsungen AG 34209 Melsungen
Combitrans Set Mod.II Uni Gießen	BiBraun Melsungen AG		B.Braun Melsungen AG 34209 Melsungen

Material	Company	Unit	Address of the company
Polyethylene Tubing	Portex®Fine Bore Polythene Tubing 30m,0.58mm ID,0.96mm OD		Smith Medical ASD, Inc.Keene, USA
Water bath	Haake 83	Haake 83 DC 30	Thermo Haake GmbH Dieselstr. 4,D -76227 Karlsruhe
Isofluran pump	Dräger	ARDB -0715	Dräger Safety AG & Co. KGaA Revalstraße 1, 23560 Luebeck
Perfusor®VI	BiBraun Melsungen AG		B.Braun Melsungen AG 34209 Melsungen
Millex®GP Filter	Millex®GP	0.22 µm	Millipore Corporate Headquarters290 Concord Rd. Billerica, MA 01821 USA
Magnetic stirrer bar	IKA -Combimag RCT		IKA® Werke GmbH & Co. KG Janke & Kunkel -Str. 10, D -79219 Staufen
Laser Flow BRL -100	BRC Bio Research Center Co.,Ltd		BRC Bio Research Center Co.Ltd. 4F Yokota Bldg. 2 -28 24 Izumi Higashi -ku Nagoya 461 -0001 Japan
Ventilator pump	Dwyer USA	SAR -830/PVentilator	SAR -830/PVentilator Dwyer Instruments Inc. P.O. Box 373, 102 Indiana Hwy. 212, Michigan City, IN, 46361 USA
Glucometer	Bayer Health care	Glucometer elite XL	Bayer vital GmbH, 51368 Leverkusen
Ascensia®Elite Sensor	Bayer Health care	1x100 articles	Bayer vital GmbH, 51368 Leverkusen
Lactate device	Arkray	Lactate Pro	Arkray Inc. 57 Nishi Aketa -Cho, Higashi Kujo, Minami -Ku Kyoto Japan
Lactate Pro®Test Strip	Arkray	1x25 articles	Arkray Inc. 57 Nishi Aketa -Cho, Higashi Kujo, Minami -Ku Kyoto Japan
Blood gas analyzer,Rapidlab™ 348	Bayer Health care		Bayer vital GmbH, 51368 Leverkusen
Thermostate	Alfos	PT 100	Alfos AG, 4105 Biel-Benken
Electrocautery	Aaron	Aaron 900,	Aaron Medical 7100

Material	Company	Unit	Address of the company
		High Frequency Desiccator	30th Avenue N. St. Petersburg, FL 33710
Dremel®	Dremel Europe	Dremel Moto - flex 250 Watt 22.000 rounds	Dremel Europe Kortijnenberg 60 Breda-NL
Lamp	Olympus europe	Highlight 3100	Olympus Germany GmbH Wendenstr. 14 -18 20097 Hamburg
Surgical lamp	Original Hanau		Original Hanau Quarzlampen GmbH
Computer for analyzis	Pentium III, Windows 98		
Amplifier 1	WPI	Transbridge 4 M	World Precision Instruments 175 Sarasota Center Boulevard Sarasota, FL 34240 9258
Amplifier 2	HSE		HUGO SACHS ELEKTRONIK HARVARD APPARATUS GmbH Gruenstrasse 1 D 79232 March-Hugstetten
Analyzing software	HSE		HUGO SACHS ELEKTRONIK HARVARD APPARATUS GmbH Gruenstrasse 1 D 79232 March-Hugstetten
Rat IFN-γ ELISA Set	BD Biosciences Pharmingen		BD Biosciences Pharmingen 10975 Torreyana Road San Diego, CA 92121
Rat TNF ELISA Set	BD Biosciences Pharmingen		BD Biosciences Pharmingen 10975 Torreyana Road San Diego, CA 92121
Rat IL 10 ELISA Set	BD Biosciences Pharmingen		BD Biosciences Pharmingen 10975 Torreyana Road San Diego, CA 92121
Enhanced chemiluminescence (ECL) kit	Amersham		Amersham, USA
ImProm-II™ Reverse transcription System	Promega		Promega, USA

Material	Company	Unit	Address of the company
Milk powder	Roth		Roth, Germany
N,N´-methylene-bis-Acrylamide solution	Roth		Roth, Germany
Protein rainbow markers	Amersham		Amersham, USA
RIPA buffer	Santa Cruz		Santa Cruz, USA
SDS solution,10% q/v	Promega		Promega, USA
SYBR® GreenER™ qPCR SuperMixes Universal kit			Invitrogen, USA
Tris-HCl 0.5 M, pH 6.8			Amresco SOLON, USA
Tris-HCl 1.5 M, pH 8.8			Amresco SOLON, USA
Trizol	Invitrogen		Invitrogen, USA
UltraPure water			Cayman Europe, Estonia
96-well microplate			Corning, USA
AGFA cronex 5 medical X-ray film			AGFA, Belgium
Film casette			Kodak, USA
Filter tips(10,100,1000µl)			Nerbe plus, Germany
Gel blotting paper			Whatman, USA
Nitrocellulose membrane			Pall Corparation, USA
Tips (10,100,1000µl)			Eppendorf, USA
BioDoc Analyzer			Biometra, USA
Electrophoresis chamber			Biometra, USA
Freezer(+4°C,-20°C,-80°C)			Bosch, Germany
PCR-thermocycler			Biometra, USA
Shaker			Biometra, USA
Western blot unit			Biometra, USA
Vortex machine			VWR, Germany
Anti foam 204	Sigma-Aldrich		Steinheim, Germany

Material	Company	Unit	Address of the company
Hydrochloric acid	Merck		Merck, Darmstadt, Germany
Sodium hydroxide 1N	Merck		Merck, Darmstadt, Germany
Sodium nitrite	Sigma-Aldrich		Steinheim, Germany
Sterile isotonic saline solution (0.9% NaCl)	Braun		Braun, Melsungen, Germany
Vanadium chloride	Sigma-Aldrich		Steinheim, Germany
Microfilter Syringes	Hamilton Bonaduz AG	10 µl	Hamilton Bonaduz AG, CH-7402 Switzerland
Nitric Oxide Analyzer (NOA) Sievers 280	Foehr Medical Instruments		Foehr Medical Instruments, Seeheim, Germany
NoaWin 32 Software	DeMeTec		DeMeTec, Langgöns, Germany

3. RESULTS

Ventilation was uninterrupted and oxygen supply was controlled, therefore, blood gas analysis of pO_2 and pCO_2 did not change significantly. pCO_2 levels were constant around 35-40 mmHg. The data are given in the tables as follows: Table 3 illustrates the group averaged data for glucose, lactate, and pH, partial pressure of oxygen and carbon dioxide as well as hemoglobin content, which were obtained at baseline conditions (baseline) and at the end of the experiment (end). Table 2 and 4 present the group data for mean blood pressure together with N2-P1 potential amplitude, P1 latency, the evoked flow velocity response and resting LDF signal for septic and non septic animals. Laboratory findings are presented as followed:

Figure 11: Data for mean arterial blood pressure (BP), SEP, evoked hemodynamic responses (EVFR), and resting laser-Doppler flow values (resting LDF); Figure 12: Cytokine concentrations of TNF-α, IFN-ɣ, IL-6, and IL-10 in plasma samples; Figure 13: NO-signalling by qRT-PCR and western blot analysis of iNOS expression in the cortex; Figure 14: Western blot analysis and quantification of HIF 2 α expression in the cortex ; Figure 15: Real time PCR BAX mRNA expression in the cortex 4.5h after LPS administration for all LPS groups and the control group.

3.1. Vagal effects on clinical and neurofunctional data in non-septic rats

In non-endotoxinemic groups, VGX and VGX+STIM did not significantly change clinical or neurofunctional data as compared to the baseline. In response to stimulation of the left nervus vagus no significant blood pressure decrease was induced: SHAM 116±20 mmHg vs. 108±20 mmHg; VGX 115±13 mmHg vs. 115±22 mmHg; VGX+STIM 109±10 mmHg vs. 93±21 mmHg (Table 2).

pH level was higher than the physiological level. The higher pH across all experimental groups was related to the α-chloralose anaesthesia which leads to a well-known metabolic alkalosis effect: SHAM 7.49±0.06 vs. 7.47±0.03; VGX 7.45±0.05 vs. 7.50±0.06; VGX+STIM 7.52±0.06 vs. 7.51±0.04. Similar to the SHAM group and due to the volume administration, hemoglobin levels decreased moderately until the end of experiments in each group (VGX 140±10 g/l vs. 130±10 g/l and VGX+STIM 130±10 g/l vs. 100±20 g/l, respectively, both $p<0.05$; Table 3).

Glucose levels were stable throughout the experiment (SHAM 63±8 mg/dl vs. 84±21 mg/dl; VGX 98±30 mg/dl vs. 98±18 mg/dl; VGX+STIM 71±15 mg/dl vs. 105±49 mg/dl, Table 3) as well as lactate levels (SHAM 0.8±0.05 mmol/l vs. 0.9±0.1; VGX 0.8±0.03 mmol/l vs. 0.9±0.1; VGX+STIM 0.9±0.2 mmol/l vs. 1.3±0.5, Table 3).

		Baseline	30min	60min	120min	180min	240min	270min
Mean BP (mmHg)	SHAM	116±20	120±12	108±20	113±14	114±19	108±20	108±20
Mean BP (mmHg)	VGX	115±13	110±13	112±19	109±14	110±17	115±22	115±22
Mean BP (mmHg)	VGX+STIM	109±10	99±14	103±18	100±23	104±29	93±21	93±21
SEP (μV)	SHAM	13±7	15±6	14±4	15±5	14±5	15±5	14±5
SEP (μV)	VGX	15±9	15±8	16±9	16±9	15±6	15±6	16±8
SEP (μV)	VGX+STIM	15±9	13±4	14±4	12±5	11±5	13±3	15±8
P1 latency (ms)	SHAM	10,8±1	11,1±1	11,2±1	11,1±1	11,3±1	11,4±1	11,7±2
P1 latency (ms)	VGX	10±0,6	10±0,5	10±0,6	10±0,4	10±0,4	10±0,4	10,1±0,5
P1 latency (ms)	VGX+STIM	10,2±1	10,4±1	10,5±1	10,3±1	10±0,7	10±0,7	10±0,9
EFVR (%)	SHAM	34±10	26±7	30±11	31±15	29±14	31±12	28±7
EFVR (%)	VGX	23±13	23±15	21±11	24±15	24±6	23±7	24±11
EFVR (%)	VGX+STIM	33±13	35±18	36±13	29±17	31±18	32±25	38±14
Resting LDF (U)	SHAM	163±66	152±71	140±62	145±82	142±75	145±71	139±72
Resting LDF (U)	VGX	233±78	219±106	211±88	199±84	203±101	213±111	201±107
Resting LDF (U)	VGX+STIM	224±92	231±75	232±60	239±30	193±33	196±49	186±57

Table 2: Group averaged data for mean blood pressure, somatosensory evoked potentials, P1 latencies, evoked flow velocity responses and resting LDF signal at the different time points of the experiment. Data are given as the mean ± standard deviation (SD) together with statistical differences. BP=blood pressure; EFVR=evoked flow velocity responses; LDF=Laser-Doppler flowmetry; SEP=somatosensory evoked potentials; SHAM=sham surgery; VGX=bilateral vagotomy; VGX+STIM=bilateral vagotomy and distal vagus nerve stimulation.

Evoked flow velocity responses were reduced slightly but not significantly only in SHAM group compared to baseline (34±10% vs. 28±7%, Table 2). There were no signs of cerebral hyperaemia in these groups, too. SEP remained the same in the non-endotoxinemic groups as well as the P1 latency, which stayed around 10-11 μV (Table 2).

	Glucose (mg/dL		Lactate (mmol/L)		ph		p02(mmHg)		pC02 (mmHg)		Hemoglobin(g/l)	
	Base	End	Base	End	Base	End	Base	End	Base	End	Base	End
SHAM	63±8	84±21	0,8±0,05	0,9±0,1	7,49±0,06	7,47±0,03	250±18	246±29	36±3	38±4	140±10	120±20**
VGX	98±30	98±18	0,8±0,03	0,9±0,1	7,45±0,05	7,50±0,06	265±19	250±23	41±8	33±4	140±10	130±10*
VGX+STIM	71±15	105±49	0,9±0,2	1,3±0,5	7,52±0,06	7,51±0,04	259±19	248±5	37±5	36±5	130±10	100±20*
SHAM LPS	65±13	69±26	0,8±0,1	1,9±0,5^{S}	7,47±0,05	7,45±0,03	250±14	233±30	40±4	35±3*	150±10	120±10^{S}
VGX LPS	82±22	129±90	0,8±0,1	2,2±0,7^{S}	7,45±0,07	7,37±0,08**	272±13	249±26	41±6	39±4	150±10	120±20**
LPS+STIM	85±25	65±20	0,9±0,1	1,8±0,6***	7,48±0,4	7,43±0,1	251±22	233±21	38±2	35±5	130±10	100±20***

Table 3: Group averaged data for glucose, lactate, pH, $p0_2$, $pC0_2$ and hemoglobin. Data are given as the mean± standard deviation (SD) together with statistical differences. Significance is given as: * $p<0.05$; ** $p<0.01$; *** $p<0.001$; ^{S} $p<0.0001$ compared with baseline. $pC0_2$=partial pressure of carbon dioxide; SHAM=sham surgery; LPS=lipopolysaccharide; VGX=bilateral vagotomy; VGX+STIM=bilateral vagotomy and distal vagus nerve stimulation.

3.2. LPS effects on clinical and neurofunctional data in non treated endotoxinemic rats

No rats died from 5 mg/kg LPS injection during the experiment, because it was injected slowly within 5 minutes, which prevented anaphylactic shock. Compared to the control animals, LPS-treated animals developed signs of a moderate sepsis-like syndrome with typical changes in blood pressure (SHAM LPS: baseline 123±11 mmHg vs. 90±18 mmHg, $p<0.0001$, Table 4), occurrence of metabolic acidosis by pH-level (SHAM LPS: baseline 7.47±0.05 vs. 7.45±0.03, Table 3), increase of lactate concentrations (SHAM LPS: baseline 0.8±0.1 mmol/l vs. 1.9±0.5 mmol/l, $p<0.0001$, Table 3). Hemoglobin levels dropped similarly from 150±10 g/l to 120±10 g/l, $p<0.0001$.

Neurological parameters tended to decline in function during sepsis as well. The evoked flow responses declined to 12±8%, which made 15% difference from the baseline (EFVR 27±11% vs. 12±8%, $p<0.05$, Table 4). Similarly SEP fell from 17±5 µV to 10±6 µV, $p<0.01$ (Table 4). In addition P1 latency showed a levelling off at 10 ms.

3.3. Vagal effects on clinical and neurofunctional data in VGX and VGX+STIM endotoxinemic rats

All vagotomized and vagus nerve stimulated rats survived injection of 5 mg/kg LPS. They also developed signs of a moderate sepsis-like syndrome with typical changes in blood pressure (VGX LPS: baseline 117±9 mmHg vs. 97±10 mmHg, $p<0.01$; VGX LPS+STIM: baseline 119±13 mmHg vs. 90±14 mmHg, $p<0.001$, Table 4, Figure 11A).

Compared to the SHAM LPS group, lactate levels of VGX LPS-group rose significantly to 2.2±0.7 mmol/l ($p<0.0001$), what was more than the stimulated group (VGX LPS+STIM 1.8±0.6 mmol/l, $p<0.001$). In vagotomised animals, a considerable occurrence of metabolic acidosis was observed at the end of the experiment, which was significant compared to baseline (pH: 7.45±0.07 vs. 7.37±0.08, $p<0.01$, Table 3). Hemoglobin values were increased in both groups as well (VGX LPS: baseline 150±10 g/l vs. 120±20 g/l, $p<0.01$; VGX LPS+STIM: baseline 130±10 g/l vs.100±20 g/l, $p<0.001$).

EFVR and SEP declined by the VGX group and remained stable in the VGX+STIM group.

		Baseline	30min	60min	120min	180min	240min	270min
Mean BP (mmHg)	SHAM	116±20	120±12	108±20	113±14	114±19	108±20	108±20
Mean BP (mmHg)	SHAM LPS	123±11	118±14	106±15**	104±10**	90±12^{s}	90±18^{s}	90±18^{s}
Mean BP (mmHg)	VGX LPS	117±9	109±17	91±17^{s}	94±18***	101±13*	97±10**	97±10**
Mean BP (mmHg)	VGX LPS+STIM	119±13	114±12	94±17*	92±7***	86±20^{s}	90±14***	90±14***
SEP (µV)	SHAM	13±7	15±6	14±4	15±5	14±5	15±5	14±5
SEP (µV)	SHAM LPS	17±5	16±6	15±6	12±6*	11±5*	11±4**	10±6**
SEP (µV)	VGX LPS	18±6	15±4	14±5	12±4**	11±7**	10±5**	8±5***
SEP (µV)	VGX LPS+STIM	18±8	18±9	19±9	16±5	16±5	14±4	15±7
P1 latency (ms)	SHAM	10,8±1	11,1±1	11,2±1	11,1±1	11,3±1	11,4±1	11,7±2
P1 latency (ms)	SHAM LPS	10±0,5	10±0,6	10±0,5	10±0,6	10±0,6	10,3±0,7	10,4±1
P1 latency (ms)	VGX LPS	10±0,8	10,4±1	10,4±0,8	10,6±0,4	10,6±0,7	11±0,9	11±1
P1 latency (ms)	VGX LPS+STIM	10±0,4	10±0,3	10±0,3	10±0,3	10±0,4	10,2±0,4	10±0,4
EFVR (%)	SHAM	34±10	26±7	30±11	31±15	29±14	31±12	28±7
EFVR (%)	SHAM LPS	27±11	29±11	26±8	18±10	18±16	14±11*	12±8*
EFVR (%)	VGX LPS	34±9	36±7	26±5	19±9**	17±16**	7±5^{s}	7±4^{s}
EFVR (%)	VGX LPS+STIM	34±8	35±11	32±9	31±13	28±12	29±13	28±13
Resting LDF (U)	SHAM	163±66	152±71	140±62	145±82	142±75	145±71	139±72
Resting LDF (U)	SHAM LPS	202±56	198±64	186±64	189±72	204±96	215±104	250±105
Resting LDF (U)	VGX LPS	160±70	141±58	151±62	157±57	192±60	198±67	196±59
Resting LDF (U)	VGX LPS+STIM	173±68	165±69	177±69	185±65	227±35	231±56	227±52

Table 4: Group averaged data for mean blood pressure, somatosensory evoked potentials, P1 latencies, evoked flow velocity responses and resting LDF signal at the different time points of the experiment. Data are given as the mean ± standard deviation (SD) together with statistical significances. Significance is given as: * $p<0.05$; ** $p<0.01$; *** $p<0.001$; ^{S} $p<0.0001$ compared to baseline. Data are given as the mean± standard deviation (SD) together with statistical significances.

3.4. Comparison of therapy regimes

The inflammatory response tended to be mitigated in the stimulated group (VGX LPS+STIM) whereas an opposite effect was noted in the vagotomised one (VGX LPS). Both vagal interventions did not have a significant effect on changes in the mean arterial blood pressure (mean BP, Figure 11A) or resting LDF (Figure 11D). However, SEP amplitudes (SEP, Figure 11B) and evoked flow velocity responses (EFVR, Figure 11C) were stabilized under vagal stimulation while an opposite effect was seen in the vagotomised group (Table 4). In the SHAM LPS group, EFVR significantly declined 240 min after LPS application with the smallest responses at the end of the experiments (SHAM LPS: 4.5 h: 12±8% vs. baseline: 27±11%, p=0.05, Table 4). On the one hand a stronger and earlier (120 min) lowering of EFVR was seen in the vagotomised group (VGX LPS: 4.5 h: 7±4% vs. 34±9%, p<0.0001, Table 4). On the other hand stimulated group stabilized hemodynamic responses throughout the study (VGX LPS+STIM: 4.5 h: 28±13% vs. 34±8%, p=n.s.). Similarly, the same group stabilized evoked potential amplitudes under inflammatory conditions (VGX LPS+STIM: 4.5 h: 15±7 µV vs. baseline: 18±8 µV, p=n.s., Table 4) whereas the SHAM LPS group showed a significant decline (SHAM LPS: 4.5h: 10±6 µV vs. baseline: 17±5 µV, p<0.01, Table 4). The first significant drop compared to the baseline occurred 240 min after LPS application in the SHAM LPS group (Table 4). Again, the vagotomised group showed a stronger and earlier (120 min) significant decline in potential amplitudes (VGX LPS: 8±5 µV vs. 18±6 µV, p<0,001, Table 4). The P1 latencies did not differ with time or between groups (Table 4). The occurrence of cerebral hyperaemia as concluded from the resting flow velocity recordings was approximately 30% among all endotoxinemic groups (Figure 11D, Table 4). In contrast to the non-septic rats cerebral blood flow increased gradually after sepsis induction. While systemic hypotension occurred in the endotoxinemic groups there was a considerable increase of the cerebral blood flow (Figure 11D) and drop of the evoked blood flow (SHAM LPS and VGX LPS).

Comparing the VGX LPS and VGX LPS+STIM group at each time point, there was a significant difference in the EFVR after 180 min, whereas the SEP amplitudes first differed at 4.5 h. These data indicate that uncoupling precedes changes in evoked potentials. Similarly, comparing the VGX LPS+STIM and the SHAM LPS groups a significant decline in EFVR in the SHAM LPS group occurred at 4.5 h, while the potential amplitudes did not differ between the groups at this time point.

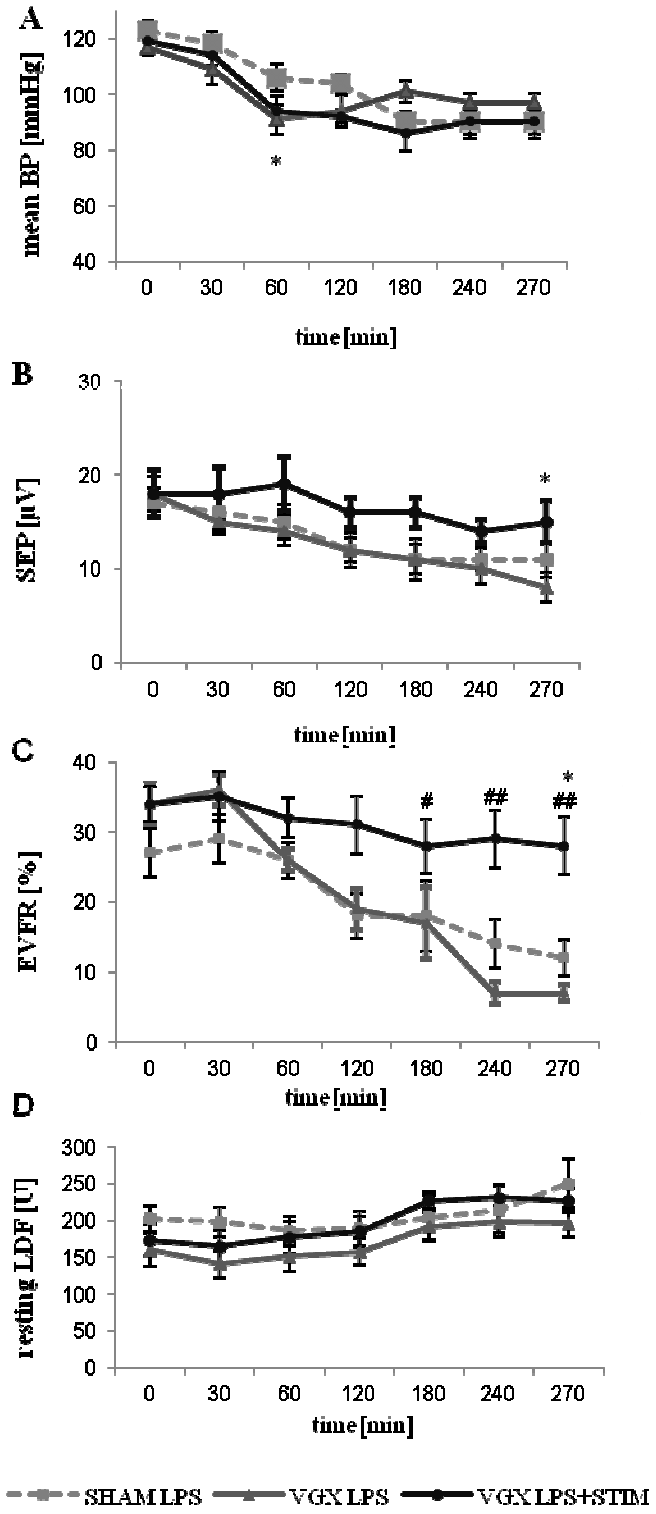

Figure 11: Data for mean arterial blood pressure (BP, (A)), somatosensory evoked potential amplitudes (SEP, (B)), evoked hemodynamic responses (EVFR, (C)), and resting laser-Doppler flow values (resting LDF, (D)) are given for the LPS treated groups. There were no significant differences for the BP and resting LDF between the groups. The resting LDF increased approximately 30% until the end of experiments. Vagus nerve stimulation stabilized potential amplitudes (VGX LPS+STIM; * $p<0.05$ vs. SHAM LPS, graph B) whereas vagotomy had an opposite effect (VGX LPS) as compared to the sham

surgeries (SHAM LPS). The evoked responses remained stable throughout the experiments in the VGX LPS+STIM group showing a significant difference to the SHAM LPS group (* $p<0.05$, VGX LPS+STIM vs. SHAM LPS, graph C). Again, vagotomy had a negative effect on the uncoupling ($^{\#}$ $p<0.05$, VGX vs. VGX LPS+STIM, $^{\#\#}$ $p<0.01$, VGX vs. VGX LPS+STIM, graph C). n=10 rats each. Data are given as the mean ± SEM.

3.5. Vagal effects on cytokines in septic rats

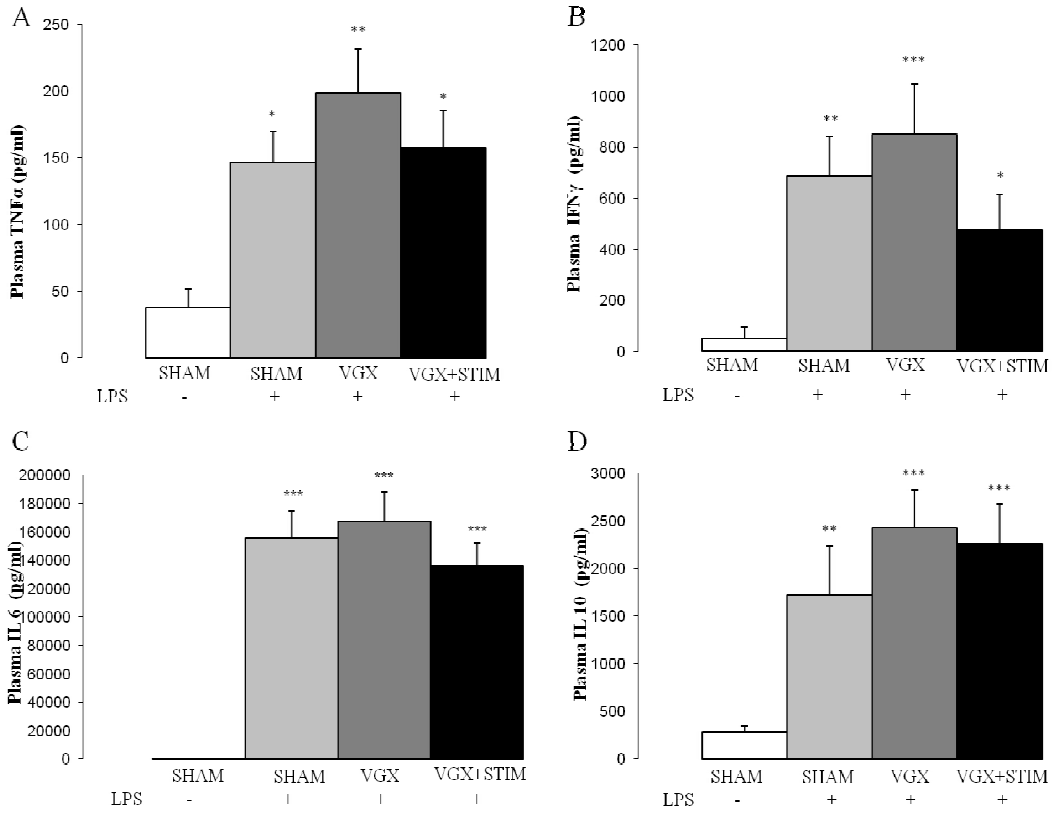

Figure 12. Cytokine concentrations in plasma samples 4.5h after LPS administration for all LPS groups and the control (SHAM, white bar) group. (A) TNF-α, (B) IFN-ɣ, (C) IL-6, and (D) IL-10 levels measured by ELISA. In all groups a significant increase occurs under septic conditions. Although vagus nerve stimulation (VGX LPS+STIM; black bar) appears to have an anti-inflammatory action, while vagotomy (VGX, gray bar) has a pro-inflammatory action, statistical examinations between the groups were insignificant. Statistical differences versus SHAM are given as * $p<0.05$; ** $p<0.01$; *** $p<0.001$; n=6 rats in each group. Data are given as the mean ± SEM.

Compared to SHAM, TNF-α, IFN-ɣ, IL-6 and IL-10 levels in plasma samples 4.5h after LPS administration measured by ELISA were increased significantly under septic conditions. Interestingly, vagus nerve stimulation appears to have an anti-inflammatory action, while vagotomy has a pro-inflammatory action, however statistical examinations between the groups were insignificant. A trend towards decreased inflammation levels by vagal stimulation and increased levels in vagotomised animals was observed (Figure 12).

3.6. Vagal effects on NO signalling in septic rats

NO signalling was analysed on mRNA and protein level from cortex tissue as well as on plasma level using nitrite and nitrate determination method 4.5 hours after intravenous LPS-injection (Figure 13). Although there were no major differences of iNOS mRNA expression within the LPS groups, there was a significant increase in the protein levels as shown by western blot analysis. The endotoxinemic groups vagotomy (VGX LPS) and vagus nerve stimulation (VGX LPS+STIM) showed a further significant increase in NO signalling as compared to SHAM LPS ($^{\#}$ $p<0.01$ VGX LPS+STIM vs. SHAM LPS; $^{\$}$ $p<0.001$ VGX LPS+STIM vs. SHAM LPS; Figure 13B).

Nitrite and nitrate levels rose sharply in all sepsis groups. Interestingly, they were significantly lower in the VGX LPS group as compared to the other two LPS groups (Figure 13C).

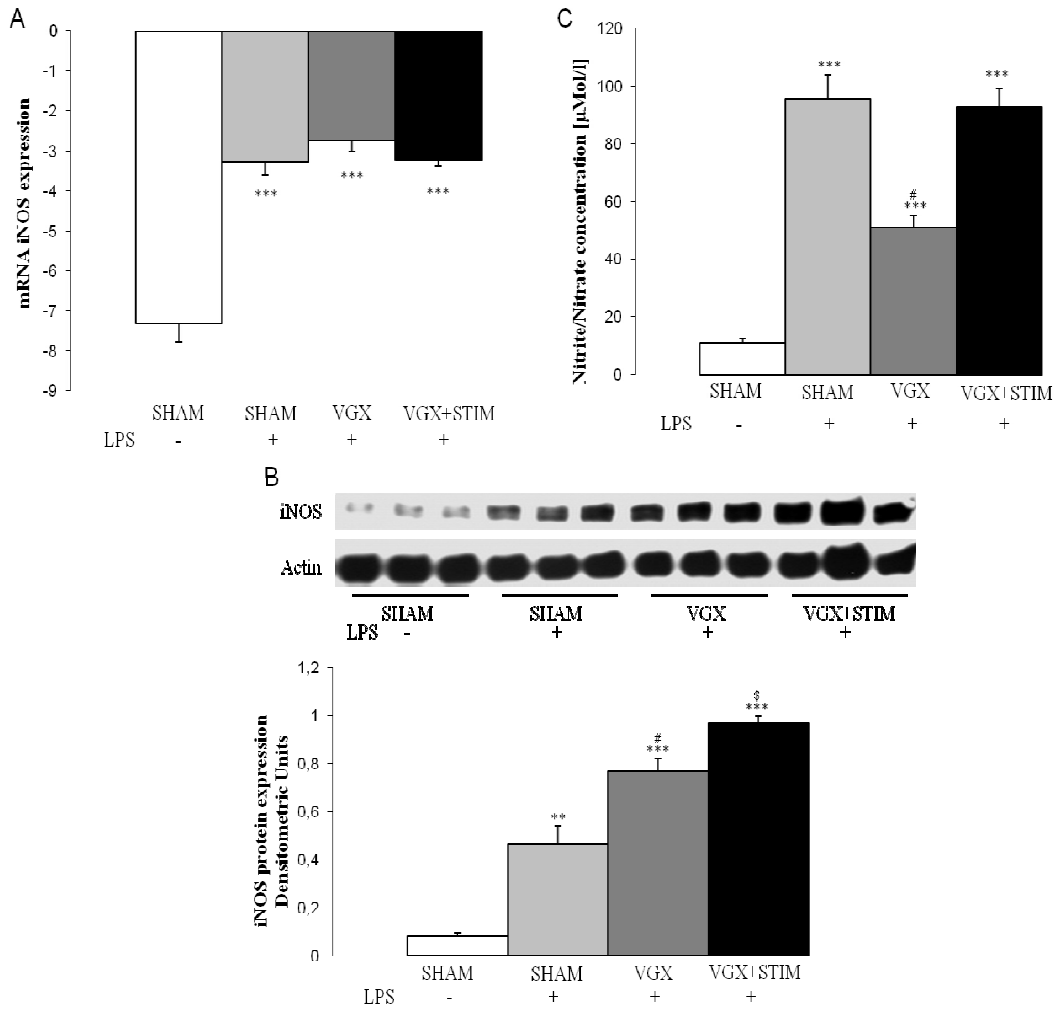

Figure 13. Real time PCR iNOS mRNA expression (graph A), western blot analysis, and protein qualification of iNOS expression (graph B) in rat cortexes 4.5h after LPS administration for all LPS groups and the control group (SHAM, white bar). Graph C shows the results of the plasma nitrate/nitrite quantification from sampels taken 4.5h after LPS administration. Besides a significant increase in the mRNA expression in all LPS groups (* $p<0.05$, ** $p<0.01$ vs. SHAM, graph A) there were no differences comparing the vagotomy (VGX LPS, gray bar), LPS-treated and sham-operated (SHAM+LPS, light gray bar) or vagus nerve-stimulated (VGX LPS+STIM, black bar) groups (n=6 rats). All LPS groups showed a significant increase in iNOS protein compared to SHAM. Within the LPS groups, vagotomy (VGX LPS, gray bar) and vagus nerve stimulation (VGX LPS+STIM, black bar) led to a further significiant increase compared to SHAM LPS (light gray bar). ** $p<0.01$, *** $p<0.001$ compared to SHAM, $^{\#}$ $p<0.01$ VGX LPS+STIM vs. SHAM LPS, $^{\$}$ $p<0.001$ VGX LPS+STIM vs. SHAM LPS. n=3 rats each. Nitrite/nitrate significantly increased in all LPS groups compared to SHAM. Compared to SHAM LPS (light gray bar) and vagus nerve stimulation (VGX LPS+STIM) the VGX LPS (gray bar) group showed significantly lower values. *** $p<0.001$ compared to SHAM; $^{\#}$ $p<0.001$ compared to SHAM. n=10 rats each. Data are given as the mean ± SEM.

3.7. Vagal effects on hypoxia- and apoptosis signalling in septic rats

Western blot analysis and quantification of HIF-2α expression in the cortex 4.5h after LPS administration for all LPS groups and the control group is shown in Figure 14. HIF-2α was increased significantly only in the VGX LPS group as compared to the SHAM ($p<0.05$ compared to SHAM), while no significant difference was detected in the SHAM LPS and VGX LPS+STIM group. The significant increase in the VGX LPS group is an indicator of a hypoxic condition.

Analysis of apoptosis signalling molecule BAX at mRNA level showed no differences between endotoxinemic groups and control SHAM group (Figure 15).

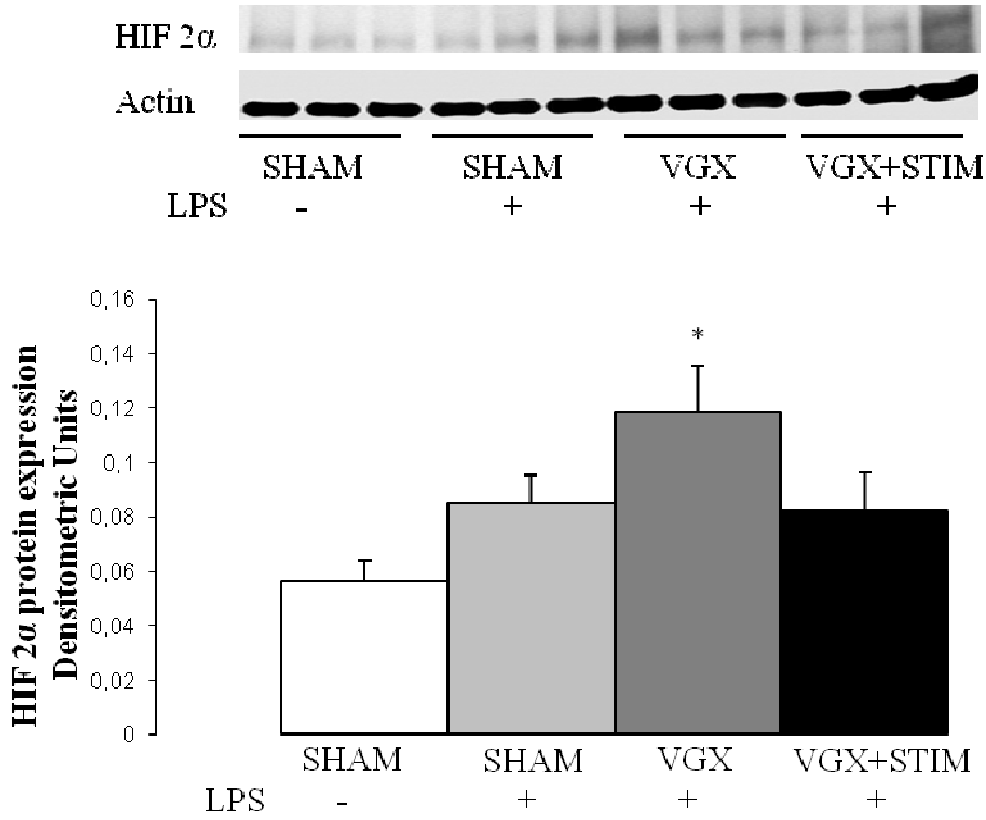

Figure 14. Western blot analysis and quantification of HIF-2α expression in the cortex 4.5h after LPS administration for all LPS groups and the control group (SHAM, white bar). With the exception of the vagotomy group (VGX LPS, gray bar), no significant differences to the SHAM group were found in the LPS-treated and sham-operated (SHAM+LPS, light gray bar) or vagus nerve-stimulated groups (VGX LPS+STIM, black bar). The significant increase in the VGX LPS (gray bar) group is an indicator of a hypoxic condition; * $p<0.05$ compared to SHAM; n=3 rats each. Data are given as the mean±SEM.

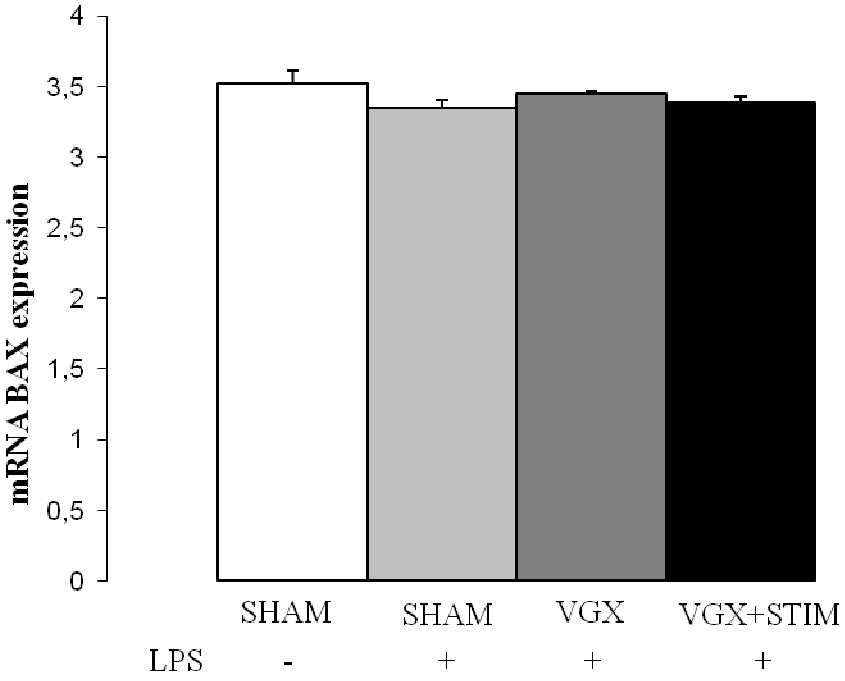

Figure 15. Real time PCR BAX mRNA expression in the cortex 4.5h after LPS administration for all LPS groups and the control group (SHAM, white bar). Compared to SHAM LPS groups did not show any differences. LPS groups with vagotomy (VGX LPS, gray bar), sham operation (SHAM+LPS, light gray bar) or vagus nerve stimulation (VGX LPS+STIM, black bar) also did not show differences. N=6 rats each. Data are given as the mean±SEM.

4. DISCUSSION

4.1. Sepsis-associated delirium

Sepsis is a major cause of death in intensive care units. There is increasing evidence that early therapeutic intervention can play a key role in improving survival after sepsis. In the early phase of sepsis, two pivotal pathogenic mechanisms trigger disease progression: a massive stimulation of the innate immune system called the cytokine storm, and NO-related progressive microcirculatory failure (Hotchkiss, Coopersmith et al. 2009; Lundy and Trzeciak 2009). Previous studies showed that microvascular dysregulation occur in patients during the early stages of sepsis. The observed abnormalities are greatest in more severely ill patients and are thought to be involved in the pathogenesis of sepsis related organ dysfunction (Trzeciak, Dellinger et al. 2007; Spanos, Jhanji et al. 2010). It has been shown that the microcirculatory failure is responsible for the first cardiac, pulmonary and gastrointestinal dysfunctions and appears before changes in the macrocirculation (Vincent and De Backer 2005; Rosengarten, Hecht et al. 2007). However further efforts to improve sepsis survival focus increasingly on intervention during its earliest stages.

Brain dysfunction occurs early in the course of systemic sepsis. The brain is susceptible to an insufficient blood supply due to strict aerobic metabolic pattering and its inability to store oxygen. Early uncoupling of the neurovascular coupling (NVC) was shown to precede changes in evoked potential amplitudes, indicating a critical role of the cerebral microcirculation in the occurrence of SAD (Rosengarten, Hecht et al. 2007). This has led to a particular emphasis on the SAD management within the first few hours of sepsis progress (Rivers, Nguyen et al. 2001).

In the last years, distal vagus nerve stimulation has evolved as a promising new therapeutic regimen mitigating the inflammatory response and improving the outcome in animal models of sepsis in early and late stages (Borovikova, Ivanova et al. 2000; Tracey 2007). However, the effects of vagus nerve stimulation on the cerebral microcirculatory function in the early stage of sepsis, as well as on NO levels, had not been investigated. Therefore, this study was primarily concerned with the role of distal vagus nerve stimulation vs. vagotomy on the integrity of the NVC in the brain by using a rat sepsis model by endotoxin-induced inflammatory syndrome. The effects on cytokine production, markers of apoptosis, hypoxia and the NO-signalling are presented

as well as the assessment of sepsis progress. Non-specific effects of both vagal interventions on the NVC were assessed in non-septic rats.

4.2. Vagus nerve as a modulator of inflammatory response

The central nervous system consists of two parts: the somatic nervous system and the autonomic nervous system (ANS). Autonomic nervous system is responsible for maintaining homeostasis like arterial pressure, gastrointestinal motility and secretion, body temperature and other activities. It consists of peripheral and central components. The peripheral component consists of ganglia and nerves distributed throughout the body and the central of centers and nuclei located in the central nervous system (CNS). The peripheral nervous system (PNS) contains efferent (or motor) neurons, which project chiefly to, and control the activity of, smooth muscle and secretory cells, and afferent (or sensory) neurons, which signal to the sensory side of the system and support both sensation and reflexes. The efferent visceromotor neurons have three subdivisions: parasympathetic and sympathetic nervous system that usually act reciprocally of each other and the enteric nervous system, which are known as autonomic nervous system.

About 75% of parasympathetic nerve fibers arise from the tenth cranial nerves, however the vagus nerves is bilateral. The vagus nerve originates in the medulla oblongata and travels all the way through the cervical area to the thoracic and abdominal regions of the body. It supplies parasympathetic innervations to the heart, the lungs, the esophagus, small intestine, the proximal half of the colon, the liver, the pancreas, and the ureters. It consists of preganglionic neurons. However, the preganglionic fibers travel uninterrupted to their destination and synapse with postganglionic neurons inside or near the target organ where short postganglionic fibers spread throughout the organ.

The brain receives information from the immune system by humoral as well as neural pathways. Vagus nerves signal to the brain for danger. For example cytokines and bacterial products such as endotoxin stimulate afferent neural fibers, which proceed to the brain through the vagus nerve and result in the initiation of an acute phase response and induction of fever (Maier, Goehler et al. 1998). 80-90% of the nerve fibers in the vagus nerve are afferent (sensory) nerves communicating the state of the viscera to the brain. The neurotransmitter at the vagal presynaptic terminals is acetylcholine (Ach). Through the humoral route cytokines can signal via circumventricular organs.

Parasympathetic innervation of the heart is mediated by the vagus nerve. Specifically, the vagus nerve acts to lower the heart rate. The right vagus innervates the sinoatrial node. Parasympathetic hyperstimulation results in bradyarrhythmias after therapy. The left vagus when hyperstimulated predisposes the heart to atrioventricular (AV) blocks. However, the left vagus nerve has less cardio-depressive effects then the right one. Thus, the left vagus nerve stimulation was chosen for the current study (Berthoud 2008; Klabunde 2011).

Anti-inflammatory cholinergic effects of vagus nerve

In the last few years, electrical stimulation of the vagus nerve has been conceptualized as an alternative therapy for modulating the inflammatory response during sepsis. The mediator involved in this so-called "cholinergic anti-inflammatory pathway" is Ach, which is the neurotransmitter of sensory neurons and others. Acetylcholine putatively binds to the α7 nicotinic cholinergic receptors expressed by macrophages and other immune cell types and reduces the release of the pro-inflammatory cytokine like TNF-α. It is suggested that the spleen is involved in cytokine regulatory effect of vagus nerve stimulation. Despite intensive research and discussions about possible vagal fiber switching to the spleen, there is a considerable lack of evidence proving direct vagus nerve innervation to the spleen. Other researchers showed data that electrical vagus nerve stimulation inhibited the acute inflammatory response in acute hypovolemic hemorrhagic shock (Guarini, Altavilla et al. 2003), splanchnic artery occlusion shock (Altavilla, Guarini et al. 2006) and intestinal inflammation during experimentally induced ileus (de Jonge, van der Zanden et al. 2005). This first concept of vagal inflammatory reflex by Tracey and others did not clarify the exact mechanism of how vagal stimulation is affecting the sepsis (Borovikova, Ivanova et al. 2000; Tracey 2002; Rosas-Ballina and Tracey 2009).

By cervical bilateral vagotomy the afferent input from the entire vagus nerve to the brain is eliminated, so that the activation of the brain is interrupted. In addition bilateral vagotomy worsened the inflammation by sharply increasing TNF-α levels in the liver (Borovikova, Ivanova et al. 2000). Other studies showed, that subdiaphragmatic vagotomy blocked or attenuated plenty of brain-mediated responses to peripheral immune organs (Maier, Goehler et al. 1998).

Alternatively to vagal stimulation, the pharmacological stimulation of the α7 subunit of the nicotinic Ach receptors could be used. GTS-21 is α7nAChR-selective partial

agonist, which attenuated cytokine production and was investigated for treatment of Alzheimer´s disease. CNI-1493 similarly to GTS-21 has anti-inflammatory effect by inhibition of pro-inflammatory cytokines. In clinical studies, both CNI-1493 and GTS-21 were neither of which cross the blood brain barrier, were proven to be less effective than vagus nerve stimulation (Zheng, Wei et al. 2007; van Westerloo 2010).

The vagal immune effects, which moderate the inflammatory response and prevent tissue damage may lead to new therapeutic approaches for septic patients. The efferent vagal nerve is more relevant for further explorations than the afferent one, due to its possible direct effect on innervation of the reticuloendothelial system. Taken together, stimulation of efferent vagus nerve leads to robust stimulation of inflammatory pathways, but further investigations need to be performed to assess the overall effects.

In conclusion, neurological recordings of SEP and NVC as well as analysis of NO system, cytokines, hypoxic and apoptotic modulators contribute to our understanding of the cholinergic anti-inflammatory mechanism.

4.3. Animal model

Different experimental models exist for the reproduction of pathophysiological conditions. Likewise, *in vitro* experiments are useful complements for animal experiments including: *ex vivo* organ culture, cell culture, which can all be performed in a special medium according to their physiological milieu. However, the practical application of data obtained from *in vitro* experiments concern mainly structural and functional connections between cells and tissues. They cannot fully replicate the complexity of a systemic inflammatory response.

In contrast *in vivo* models are experiments implemented on living organisms which give researchers the opportunity to holistically analyze the complexity of the septic process. The clinical course of sepsis is usually prolonged, taking days to weeks to manifest as progressive organ failure. By contrast, the time course of illness in animal models ranges from hours to days, which intensifies the process of sepsis. This study was performed using a standardized rat animal model using established ways for measurements of NVC and SEP thereby making it a clinically relevant model.

4.4. Endotoxin/LPS animal model

This study presents pathophysiological changes similar to the sepsis associated inflammatory response in humans via an endotoxin animal model. Endotoxin models are easy to perform and relatively easy to replicate. The endotoxin animal model used in this study was already standardized for examination of neurovascular measurements occurring during sepsis (Rosengarten, Hecht et al. 2007). Administration of endotoxin to rats results in hemodynamic and biochemical abnormalities, which are like those observed during severe sepsis in humans. Endotoxin is an essential ingredient of the outer cell wall of gram-negative bacteria which initiates innate immune defense by activation of toll-like receptor-4 (TLR-4). TLR-4 cell signaling results in the transcription of inflammatory genes. Often used sepsis models are the exogenous administration of LPS intravenously, intraperitoneally, intratracheally or by CLP. In this model is used intravenous administration of 5 mg/kg LPS which replicates septicaemia. Higher doses of LPS trigger a more pronounced sepsis-like syndrome. Intravenous LPS administration can be tightly controlled with precise dosage of the endotoxin and assure fast activation of host response. On the contrary, CLP induces polymicrobic sepsis in which exactly dose can not be controlled, because it is not known exactly how many microorganisms are passing through the puncture. Here, the limitation lies in the exact timing of the abdominal translocation of the pathogen germs. For this reason, intravenous LPS injection was preferred in this animal model for examination of the inflammatory response.

In this study 5 mg/kg LPS induced more moderate sepsis-like syndrome compared with previous studies of the same animal model (Rosengarten, Hecht et al. 2007; Rosengarten, Wolff et al. 2009). The difference in sepsis severity could not be explained by difference in the endotoxin, animal body weight, narcotic regime or experimental procedure. Even though the same background was used, the rodents in this study were ordered from a different distributor, possibly affecting experimental outcome. Therefore, it is likely that the weaker response was related to differences between animal strains. However, all rats react similar to LPS-injection and developed not drastic but moderate sepsis syndrome compared to earlier investigations.

Higher LPS doses are related to more pronounced sepsis-like syndrome such as 15 mg/kg LPS showed in Borovikova's study (Borovikova, Ivanova et al. 2000). Neurological recordings are needed to be performed in this study, so higher than 5 mg/kg LPS would not allow for such measurements over a period of 4.5 hours.

Borovikova stopped experiments just 1 hour after LPS application; a much shorter duration than our experiments.

4.5. Narcosis with α-chloralose and pancuronium relaxation

α-Chloralose was chosen as anesthesia because it is believed to have a less depressive effect on cardiovascular and respiratory functions as well as on reflex activities. It is widely used as a narcotic in the neuroscience field because it provides robust hemodynamic responses to functional stimulation such as somatosensory electrical stimulation of the forepaw. Compared to other narcotics like halothane or pentobarbital used by activation of cerebral metabolic rate of glucose (CMRglc) evoked by forepaw electrical stimulation in rats, α-Chloralose effects were most similar to those performed on conscious animals (Ueki, Mies et al. 1992). Other studies confirmed that α-Chloralose is more suitable for studying local cerebral blood flow (lCBF) coupling to neuronal functional activation (Wang, Zheng et al. 2008).

Isoflurane causes both respiratory and cardiovascular depression and stimulates NO-signaling in the brain, which can influence the measurements. For this reason a washout period of one hour was allowed before the start of the experiments.

α-Chloralose leads typically to myoclonic movements and tonic extensions of the limbs; therefore animals were paralyzed with pancuronium bromide. Pancuronium paralyzes the skeletal musculature but not the vascular smooth muscle (Nakao, Itoh et al. 2001).

The use of α-Chloralose as an anesthetic is still controversial because of its long lasting analgesic properties, myoclonic effects and blood pressure effects as well as its limited reversibility. In this study, animals were sacrificed at the end of the experiments, so reversibility of narcosis was not relevant. α-Chloralose slightly induced alkalosis, but that did not impact the experiment. This combination of anesthesia was already standardized and used successfully in previous experiments using similar animal models.

4.6. Effects of VGX STIM and VGX on clinical data

In this study, neither bilateral vagotomy nor left distal vagal stimulation affected drastically the clinical data of non-endotoxinemic animals. That evidence supports the hypothesis that left vagus nerve stimulation has a less cardio-depressive effect in

regards to heart rate and mean blood pressure. Changes in haemoglobin levels were observed. However, these changes were directly caused by infusion of 0.9% NaCl plus pancuronium bromide volume administration throughout 4.5 hours measurements in the non-endotoxinemic and endotoxinemic groups.

Occurrence of clinical data changes were observed after LPS administration by rats, which were less or more severe according to the LPS-doses (Xu, Qi et al. 1993). Early recognition of hemodynamic instability in combination with the complexity of sepsis is therefore essential. In this case, doses of intravenously 5 mg/kg LPS caused a moderate sepsis-like syndrome with sepsis-related hypotension and increased lactate levels.

During sepsis, pro-inflammatory cytokines are responsible for increased synthesis of vasoactive mediators such as NO, peptide mediators and particularly prostanoids (PGI2, PGE2), which cause vasodilation. This results in diminished venous return followed by decreases in cardiac pre-load and myocardial depression. Vasoactive mediators that are released after sepsis induction cause dilatation of blood vessels and reduction of blood pressure. In this study, hypotension occured in all endotoxinemic groups, mainly caused by vasodilatatory effect of NO. In more severe cases of sepsis or later time points during septic shock, NO levels can rise from 100- to 1000-fold of normal. Consequently, it results in a disturbance of oxygen availability to organs, severe vasoplegia, myocardial depression, so that drastic derangement of microcirculatory supply occurs (Bolton, Young et al. 1993; Vervloet, Thijs et al. 1998; Spronk, Zandstra et al. 2004).

A large number of studies showed increase of blood lactate during sepsis, which is generally considered to be an indicator of inadequate oxygenation and a predictive marker of fatal outcome. The measurement of blood lactate concentrations is a widely used method to detect severity of illness as well as to monitor therapy effects. In the present study lactate served to monitor the effect of vagus nerve stimulation as a possible protective microcirculatory therapy. Lactate is formed from pyruvate by the cytosolic enzyme lactate dehydrogenase. In animal endotoxin models it was shown that lactate levels increased when oxygen consumption became dependant on oxygen delivery to the tissues, which support its anaerobic origin (Backer 2006). Cytokines, NO or endotoxin-induced functional impairment of mitochondria are responsible for the resulting inadequate oxidative metabolism. Nearly all tissues of the body rely on the aerobic metabolic pathway to produce ATP within the mitochondria in accordance with regulation of cellular homeostasis. Microcirculatory alterations are associated with

ongoing tissue hypoxia and progression of multiple organ failure. To counteract circulatory failure with impaired tissue perfusion some tissues decrease their metabolic needs or turn aerobic metabolism into anaerobic metabolism for energy requirement. Anaerobic ATP production by itself cannot fulfill the energy needs of the body. Under anaerobic conditions there is increased production of hydrogen and lactate ions, which are clinically detectable as metabolic acidosis and elevated blood lactate concentrations. Occurrence of lactic acidosis contributes to functional failure of the liver and kidneys. This outcome is associated with tissue hypoxia and can have lethal effects. Dysoxia may be the result of a defect in the cellular utilization of oxygen. In addition, some organs produce lactate more than others such as gut and lungs, which notably account for sepsis-induced hyperlactatemia. As expected, all sepsis groups in this study showed significant increases in the lactate levels after 5 mg/kg LPS administration. However, the development of metabolic acidosis was more pronounced by VGX LPS. Besides impaired tissue oxygenation, blood lactate levels could be increased by activation of glycolysis, decreased lactate clearance, hepatic insufficiency or the presence of oxygen, which reduces pyruvate dehydrogenase activity. Moreover endotoxin could deactivate the pyruvate dehydrogenase enzyme that moves pyruvate into mitochondria so that pyruvate accumulates in the cell cytoplasm where it is converted to lactate (Boldt 2002; Kruse 2002 ; Backer 2006).

However, clinical parameters such as BP and lactate concentrations are indirect clinical markers of systemic blood flow, which alone are unreliable estimates of overall hemodynamic status during critical illness.

4.7. Effects of VGX STIM and VGX on neurological data

Microcirculatory failure in the brain under septic condition is less clear. In previous studies it was shown that measurements of SEP and latency via electroencephalogram (EEG) as well as neurovascular coupling and resting flow velocity recording via LDF could be an early prognostic indicator of the systemic inflammatory response. Changes in SEPs are sensitive markers for diagnosis of SAD which allow assessment of severity and possible outcome of sepsis. It was shown that SEP amplitudes and related EFVR of the neurovascular coupling dropped when macrocirculation was still intact (Rosengarten, Hecht et al. 2007). Another technique for detection of early microcirculatory brain dysfunction is magnetic resonance imaging (MRI). MRI-

technique was used as a sensitive parameter, but there was no detection of subtle brain edema 3.5 hours after sepsis induction. Furthermore, neurovascular coupling mechanism and SEP are more reliable for detection of early cerebral dysfunction (Zauner, Gendo et al. 2002; Ohnesorge, Bischoff et al. 2003; Rosengarten, Walberer et al. 2008).

The dynamic of neuronal brain activity could be detected by techniques such as EEG and magnetoencephalogram (MEG), which are able to follow changes in neural activity on a millisecond time-scale. MEG has a poor sensitivity to the radial component of any source while EEG is equally sensitive to both radial and tangential source orientations. However EEG recording has a stronger sensitivity to electric conductivity and is technically easy to replicate by rats compared to MEG.

However, functional magnetic resonance imaging (fMRI) as a technique reflects the blood dynamics through the entire brain using effects of blood oxygenation level dependent (BOLD). fMRI has high spatial resolution (13 mm) while temporal resolution is about a second which perform a less invasive measurement technique of neural activity (Hagler, Halgren et al. 2009).

For these reasons EEGs were used in this study for detection of neuronal activity changes. Additionally the same electrical stimulation was used to analyze blood flow changes in sepsis by LDF. In this way, SEP alterations could be analyzed and defined at the same time as coupling or uncoupling of the cerebral blood flow nearly from the same cortical area. SEPs are performed from EEG-recording via electrical stimulation connected to computer. EFVR and resting flow velocity changes are measured by LDF, which has been established already as a reliable technique with high temporal and spatial resolution for measurements of flow velocity changes during sepsis. Neurodyn software was used for the analyses, and results were transferred into Excel for statistical analyses, as in previous studies (Rosengarten, Lutz et al. 2003; Rosengarten, Hecht et al. 2007).

Somatosensory potentials may be evoked by contralateral electrical stimulation of the forepaw or hindlimb of the rat. In this study the right forepaw stimulation was performed as it was evaluated already from previous studies and as it conforms closely to brain location of most intensive evoked responses. In addition, the hindlimb was cannulated for drug administration and BP recording. Activation of the somatosensory cortex can be performed not only by forepaw or hindpaw electrical stimulation, but also by whiskers or vibrissae stimulation on rat's face. Stimulation activates contralateral

neurons in the rat cortex, which correspond to an increased blood flow into the area in the brain called the barrel cortex. Laboratory rats are nocturnal (night-active) animals, which use their sensitive whiskers to explore the environment (Cox, Woolsey et al. 1993; Mirabella, Battiston et al. 2001). However whisker stimulation cannot be transferred to humans as our facial hair does not functionally correlate to rat whiskers. Taken together, forepaw stimulation qualifies for investigation of neurovascular coupling mechanism and evoked potentials alterations during sepsis.

The brain is a sensitive organ that reacts immediately against inadequate blood supply by inducing systemic inflammation. Microcirculatory disturbances after sepsis induction prevents constant glucose and oxygen supply to the cells, which resulted in energy deficiency and break down of the membrane potential. This results in nerve cell dysfunction as seen in prolonged latencies of SEP responses. Latency gives information about the time needed for the cortical nerve cell reaction after stimulus of peripheral nerve. During the experiment there was no replacement of the stimulation needles, which allows for precise analysis of nerve conductibility. Previous studies showed significantly prolonged latency times 4.5 hours after 5 mg/kg LPS induction, which occurred after depression of evoked potentials (Rosengarten, Hecht et al. 2007). However measurements of latencies in the LPS-groups did not show significant increase of nerve conductibility within systemic inflammatory process. This might be related to the less severe inflammation in the present animal model.

Resting flow velocity was analyzed for detection of cerebral hyperaemia. In contrast to previous studies where the flow velocity level was approximately 50% higher at the end of experiments, in this study cerebral hyperaemia just under 30% among all endotoxinemic groups. This may have been due to the decreased severity of inflammation and the subsequent weaker induction of iNOS signalling. In previous investigations NO-related hyperaemia was shown to exist by administration of selective iNOS inhibitors which prevented the occurrence of cerebral hyperaemia (Okamoto, Ito et al. 1998; Rosengarten, Hecht et al. 2007).

Anti- or pro-inflammatory effects of the VGX LPS+STIM or VGX LPS observed in this study are consistent with previous studies, further corroborating the hypothesis of a “cholinergic anti-inflammatory pathway” (Tracey 2009). There were no nonspecific effects observed in the VGX LPS+STIM or VGX LPS as the non-endotoxinemic groups showed no significant changes in the neurofunctional parameters.

Previous studies report a correlation between the severity of the inflammatory process and neurovascular uncoupling by applying different doses of LPS in the same rat model (Rosengarten, Hecht et al. 2007). Higher doses of intravenous LPS triggered a more pronounced sepsis-like syndrome which led to an earlier and more severe breakdown of the NVC followed by an earlier and more pronounced lowering of SEPs. Similar results on the microcirculatory function were found in many other organ systems such as the gut, the liver, the heart, and the lung (Okamoto, Abe et al. 2000; Pullamsetti, Maring et al. 2006; Eyenga, Lhuillier et al. 2010; Dyson, Rudiger et al. 2011). Microcirculatory changes occur within several hours after sepsis-induction, initially only loosely correlated to systemic hemodynamic alterations. In addition, early microvascular alteration preceding systemic hemodynamic changes was also seen under clinical conditions (De Backer, Creteur et al. 2002).

In this study, VGX LPS+STIM prevented the occurrence of early microvascular dysfunction in the brain. Comparing both vagal interventions, a significant uncoupling of the vascular responses after 180 min was found whereas evoked potentials differed only after 4.5 hours. VGX LPS resulted in an earlier and more severe drop in both evoked hemodynamic responses and in evoked potential amplitudes, compared to the SHAM LPS treated group. VGX LPS+STIM prevented a decline both in the evoked potential amplitude and in evoked hemodynamic responses. This means that uncoupling of NVC precedes changes in evoked potential amplitudes, which is consistent with early studies (Rosengarten, Hecht et al. 2007).

An increased local inflammation and therefore metabolic rate might also reduce substrates and oxygen thereby aggravating the effects of a compromised neurovascular coupling. Anyway these positive effects of vagus nerve stimulation might party explain improved outcomes of sepsis syndromes. However, morphologic changes such as a relevant brain oedema or a breakdown of the blood brain barrier did not play a role during the first hours of the present model (Rosengarten, Hecht et al. 2008).

4.8. Effects of VGX STIM and VGX on lab chemical analysis

4.8.1. Cytokines

In the early stage of sepsis, the innate immune system is activated so that not only pro- but also anti-inflammatory cytokines are released. The cytokines released affect the microcirculation, oxygen utilization, blood brain permeability as well as glucose, protein- and neurotransmitter metabolism (Bogdanski, Blobner et al. 1999). As previous

studies reported, vagus nerve stimulation has a protective effect by decreasing pro-inflammatory TNF-α level in plasma and liver, while vagotomy, on the contrary, increased TNF-α levels and worsened inflammatory process. In addition, Borovikova and colleagues also showed that IL-10 was not influenced by VGX LPS+STIM or VGX LPS one hour after LPS-injection in endotoxinemic groups (Borovikova, Ivanova et al. 2000). That is the reason why cytokines like TNF-α, IL-6, IL-10 and IFN-ɣ were examined from plasma samples in this study. Interestingly, cytokines levels did not significantly differ within endotoxinemic groups, but rather showed a pro-inflammatory tendency in the VGX LPS group and an anti-inflammatory trend in VGX LPS+STIM group. This observation is similar to cytokine effects postulated by Borovikova and her colleagues. The anti-inflammatory action of VGX LPS+STIM might have been effectively controlled by the induction of cytokines and reactive oxygen species which can also interfere with the microcirculatory integrity (Abd El-Gawad and Khalifa 2001; Gorg, Bidmon et al. 2006). However cytokines can shift astrocytic function from a nutritive into an immunostimulating role, causing inflammation in the brain parenchyma (Gorg, Bidmon et al. 2006). Moreover astrocytes play an important role in the activation of flow coupling (Zonta, Angulo et al. 2003), so that more pronounced cytokine release in vagotomy endotoxinemic group (VGX LPS) might explain the earlier drop in evoked flow velocity responses and inappropriate blood supply to the neurons.

4.8.2. NO-signalling

After LPS induction followed by cytokine release, NO-levels increased sharply causing hypotension and dissociation of cerebral circulation. In a previous investigation it was reported that the specific iNOS inhibitor 1400W stabilized BP, NVC and prevented the incidence of cerebral hyperaemia, which supports the hypothesis for a pivotal role of NO production related to the occurrence of early vasoregulative failure. Despite consistent reports of a stabilization of the microcirculation by iNOS-inhibition, the effects on the outcome were inconsistent and in most cases negative. A possible reason is that 1400W was found to lead to a dramatic decrease in glucose levels, which only appeared in septic but not in non-septic rats. Also a related decrease in SEP occurred, which could not be compensated by systemic glucose substitution. This points to an intracellular glucose utilization disturbance. The matter needs further clarification as it was shown that NO levels can shunt intracellular mitochondrial ATP production. The

former studys results were contradicting, as high NO levels were found to inhibit the mitochondrial function, whereas blocking of the iNOS preventing increased NO levels and led to the drop in potential amplitudes (Tang, Pakula et al. 1996; Vromen, Arkovitz et al. 1996; Wray, Millar et al. 1998; Lee, Lin et al. 2005; Rosengarten, Wolff et al. 2009).

NO can be induced by pro-inflammatory cytokines such as TNF-α, IL-6, IFN-ɣ. In addition its production correlates with changes in iNOS mRNA abundance, especially at the pretranslational stage such as transcription or mRNA stability (Morris and Billiar 1994). Effects of VGX LPS+STIM and VGX LPS on NO production were analyzed on mRNA- and protein level from the cortex as well as obtained from plasma samples. Lindauer and colleagues previously reported NO acting as a permissive factor in the coupling of neuronal activation in the somatosensory cortex of rats (Dreier, Korner et al. 1995; Lindauer, Megow et al. 1999). However the current study presented evidence that the positive effect on the NVC is independent of the NO-pathway, since neither nitrite/nitrate level nor the mRNA expression level of iNOS was affected by both vagal interventions. The drastically increased iNOS protein level in endotoxinemic vagotomy-group is probably related to its pro-inflammatory effects. On the other side, higher iNOS expression in VGX LPS+STIM-treated animals contrasts with its anti-inflammatory outcome and can not explain its protective effect on evoked potentials and evoked flow velocity responses. Furthermore, there are limited reports suggesting NO induction and release by direct stimulation of the vagal nerve. Brack was one of the few researchers, who showed NO-related effects of vagus nerve stimulation on the cardiac ventricle (Brack, Patel et al. 2009). Although this issue needs further clarification, the present data demonstrate that the neuroprotective effect of VGX LPS+STIM cannot be explained simply by a decrease in NO. Moreover its protective effect seems to be restricted to the microcirculation since macrocirculatory parameters such as the BP and the cerebral hyperaemia were not significantly affected by vagal stimulation. However, during specific iNOS inhibition BP was stabilized and the development of cerebral hyperaemia was prevented, which might confirm limited VGX LPS+STIM effects on microcirculation (Rosengarten, Wolff et al. 2009). Another study showed that corticosteroids inhibit iNOS expression and NO production during inflammation not only directly through epithelial cells, but also indirectly through other cell pathways. Nevertheless, a corticosteroid-like anti-inflammatory action appears unlikely as

corticosteroids significantly reduce the nitrite/nitrate levels and iNOS mRNA expression while vagal stimulation did not (Linehan, Kolios et al. 2005).

Interestingly, NO values were observed even in non endotoxinemic animals. However, NO levels were significantly increased only in LPS-treated groups. Due to intensive discussions about possible isoflurane NO-up-regulating effects, this study performed a NO washout 1 h post isoflurane anaesthesia (Baumane, Dzintare et al. 2002; Sjakste, Sjakste et al. 2005). This short isoflurane period during preparation showed less effect on iNOS-levels in non endotoxinemic groups (unpublished data).

The result of a reduced nitrite/nitrate concentration in VGX LPS group contrasts with the pro-inflammatory action of vagotomy and the increased protein expression of iNOS. Also, in this group was observed the highest lactate level during the earliest neurological data collection point indicating a complex regulatory mechanism. However this complexity might be explained by hypoxia-related reduction of NO formation. Molecular oxygen is basic substrate for NO synthesis by NOS. The Michaelis-Menten constant of NOS isoforms are defined within the physiological tissue oxygen concentration. Le Cras even suggested that restriction of O_2 substrate might limit the production of NO in different pathological processes such as hypoxia. So, changes in the oxygen concentration may have a rapid effect on NO production (Le Cras and McMurtry 2001). Another study reports that NO production by iNOS is dependent on O_2 availability. Here was shown an example in humans who developed pulmonary hypertension by high altitude. This was mainly caused by a reduced NO production due to a drop in the pO_2 tension (Robinson, Baumgardner et al. 2008). Similar results were shown in stroke models, wherein reduced NOS-activity was found in the vital tissue of the penumbra and high NOS-activity was partly explained by increased vulnerability in ischemia area (Ashwal, Tone et al. 1998).

4.8.3. Hypoxia

Although measurements of tissue gas tension are potentially useful in critical care practice and research, they do not provide a good index of tissue well being. The dissociation of the microcirculation in areas of hyper- and hypo-perfusion and a fluctuation between states is difficult to measure (Venkatesh and Morgan 2002). It is well know that both inducible hypoxic factors HIF-1α and HIF-2α respond to hypoxia under non-inflammatory conditions. Some researchers suggest that HIF-2α responses

are even long-termed. However HIF-1α and HIF-2α are differently regulated by LPS. HIF-1α is rapidly increased under inflammatory conditions independent from normoxic or hypoxic environment. In contrast, HIF-2α is not affected by LPS under normoxic conditions (Takeda, O'Dea et al. 2010). Under inflammatory conditions, hypoxia-induced expression of HIF-2α is reduced, making HIF-2α a conservative marker of hypoxia under inflammatory conditions. Therefore, hypoxia marker HIF-2α was determined and analyzed on the protein level. Increased HIF-2α level in VGX LPS-group appeared in accordance of both hypoxic and inflammatory condition.

Takeda described even antagonistic functional properties of HIF-α isoforms in relation to NO regulation in inflammatory cells. He concluded that HIF-2α might suppress NO production by induction of arginase 1, while HIF-1α might increase NO level by iNOS induction. NO production is sensitive to reduced O_2 levels. However, this hypoxic condition may partly contribute to decreased NO-levels in plasma samples in VGX LPS-group (Takeda, O'Dea et al. 2010).

Neurons are very sensitive to a chronic disturbance in cerebral blood flow. A chronic lowering of the ideal cerebral blood flow by 10% to 20% leads to protein synthesis inhibition, activation of anaerobic glycolysis followed by release of neurotransmitters, and dysfunction of neurons within a few hours. Overall, there is less energy for metabolic processes (Hossmann 1994). Inadequate oxygen and substrate supply might influence EEG activity and cause a drop in evoked potential amplitudes. Similar responses in evoked potentials were found already in different hypoxic states of the brain, independent of inflammation. For example, Arezzo and colleagues reported changes in SEP after exposure to carbon monoxide and acrylamide. Anoxic coma after cardiac arrest also resulted in evoked potential (EP) alterations in comatose patients (Arezzo, Simson et al. 1985; Daubin, Guillotin et al. 2008). Moreover, pathological brain analysis showed that 95% of sepsis patients have diffuse cerebral ischemic damage during the course of the disease. MRIs made early detection of sepsis-related brain lesions such as microinfarcts possible, which were mainly located in the white matter (Sharshar, Annane et al. 2004; Sharshar, Carlier et al. 2007). Additionally, patients who survive sepsis give signs of typical brain changes and are clinically similar to patients with cardiac resuscitation or carbon monoxide intoxication. This was associated with cognitive and functional limitations as well as neuropsychological impairment, which was in accordance with the sepsis-induced brain lesion (Devine, Kirkley et al. 2002; Harve, Tiainen et al. 2007; Iwashyna, Ely et al. 2010). However, it

seems that observed hypoxia in VGX LPS group is more likely localized then generalized. In addition, this result is supported by clinical data, which indicate sufficient macrocirculatory and pulmonary functioning.

4.8.4. Apoptosis

To provide insight into possible early effects of vagus nerve stimulation and vagotomy on apoptotic cell death, BAX mRNA level expression was investigated. Recently, it was shown that the protein-levels of BAX- and BCL-related pro- and anti-apoptotic pathways were not induced until 8 h of sepsis induction. In addition, histological changes of BAX- and BCL-2-immunoreactive cells were first observed after 24 h (Semmler, Okulla et al. 2005). Here BAX mRNA expression was not significantly changed within endotoxinemic and non-endotoxinemic groups at that early stage of sepsis, which supports data from previous studies. Moreover this study examines and accommodates the dynamic of sepsis development. Messaris and colleagues showed mitochondrial-mediated apoptosis in the rat brain early in sepsis development. At an early stage, 6 to 12 hours after sepsis induction, BAX immunoreactivity was upregulated (Messaris, Memos et al. 2004). However in our study mitochondrial dysfunction appears more unlikely as animals were subjected to 4.5 hours of sepsis (Comim, Rezin et al. 2008). Our study confirmed previous studies showing that apoptotic parameters are still not significantly expressed 4.5 hours after LPS injection.

5. SUMMARY

Sepsis is the most frequent cause of death in all intensive care units. It is characterized as a hyper-inflammatory host response including NO-related microcirculatory dysfunction leading to catecholamine-resistant shock. It leads also to macrocirculatory disorganisation and disturbance in organ perfusion. The brain is especially susceptible to an insufficient blood supply. It has been shown that vagus nerve stimulation mitigates inflammation and possibly improves the outcome of sepsis. This study presents the effects of vagus nerve stimulation on the integrity of cerebral microcirculation.

The neurovascular coupling in the somatosensory cortex was studied in ventilated and sedated rats by applying electrical forepaw stimulation and EEG and transcranial LDF recording. In both control and endotoxinemic rats, the effect of bilateral vagotomy, vagotomy with left sided distal vagus nerve stimulation, and a sham group were compared. Resting LDF, evoked potentials and hemodynamic responses were obtained over a period of 4.5 h. Regulation of NO signalling was assessed at the end of the experiment by analysing iNOS expression and nitrite/nitrate measurements, cytokines (IFN-γ, TNF-α, IL-6, IL-10), hypoxic signalling molecules such as HIF-2α and the apoptosis molecule, Bax.

The occurrence of a cerebral microvascular failure depends on the severity of the pro-inflammatory phase of inflammation. Endotoxin induced a moderate sepsis-like syndrome with typical macrocirculatory changes such as a decrease in blood pressure and the occurrence of slight cerebral hyperaemia. Time-dependent microcirculatory dysfunction with uncoupling and depression of evoked potentials were observed. Without inhibition of NO signalling, vagal stimulation stabilized neurovascular coupling, evoked potentials and showed anti-inflammatory tendency on cytokine levels. The positive effects on evoked potential amplitudes may partly explain better outcomes of sepsis syndrome. Vagotomy contributed to severe inflammation resulting in a hypoxic state, as indicated by increased HIF-2α levels. Current results from vagus nerve stimulation and vagotomy even corroborate Tracy's hypothesis of a "cholinergic anti-inflammatory pathway".

In conclusion, vagus nerve stimulation protects against early cerebral microcirculatory failure, which has relevance for neuronal integrity. Furthermore, the effects were not related to an inhibition of NO signalling.

6. ZUSAMMENFASSUNG

Sepsis wird durch eine überempfindliche Reaktion des Wirts gekennzeichnet, die den Einfluss von Stickstoffmonoxid (NO) auf die Mikrozirkulationsstörung beinhaltet, was zu einem katecholamine-resistenten Schock führt. Es kommt auch zur makrozirkulatorischen Störung und damit verbundenen Perfusionsstörungen der Organe. Das Gehirn ist sehr empfindlich gegenüber inadäquater Durchblutung. Distale Vagusnerv-Stimulation mildert das Entzündungsgeschehen und verbessert möglicherweise das Ergebnis der Sepsis. Diese Studie stellt die Auswirkungen der Vagusnerv-Stimulation auf die Integrität der zerebralen Mikrozirkulation dar.

Hierzu wird die neurovaskuläre Kopplung vom somatosensorischen Kortex bei beatmeten und sedierten Ratten durch elektrische Stimulation der Vorderpfote, EEG- sowie transkranielle Laser-Doppler-Flussmessung erfasst. Bei den nicht-septischen und septischen Ratten wurde die Wirkung der bilateralen Vagotomie, Vagotomie mit linksseitiger distaler Vagusnerv-Stimulation und einer Placebo-Gruppe verglichen. Das ruhe LDF Signal, die evozierten Potentiale und hämodynamischen Reaktionen wurden über einen Zeitraum von 4,5 Std. gemittelt. Der Effekt auf das NO-System wurde am Ende des Experiments durch die Analyse von iNOS-Expression und Nitrit/Nitrat-Messungen erfasst sowie die Zytokine (IFN-γ, TNF-α, IL-6, IL-10), hypoxischen Signalmoleküle wie HIF-2α und Apoptose-Moleküle Bax bewertet.

Das Auftreten eines zerebralen mikrovaskulären Versagens ist von der Schwere der entzündungsfördernden Phase der Erkrankung abhängig. Endotoxin induziert ein moderates sepsis-assoziiertes Syndrom mit typischen makrozirkulatorischen Veränderungen wie z.B. Senkung des Blutdrucks und schwaches Auftreten von zerebraler Hyperämie. Des Weiteren wurden zeitabhängige mikrozirkulatorische Störungen mit Entkopplung und Depression der evozierten Potentiale beobachtet. Zusätzlich zu den entzündungshemmenden Tendenzen auf den Zytokinspiegel, stabilisiert die Stimulation des Vagusnervs die neurovaskuläre Kopplung und evozierte Potentiale ohne hemmenden Einfluss auf das Stickstoffmonoxid-System. Die positive Auswirkung auf die evozierten Potentiale könnte teilweise das Ergebnis der Sepsis erklären. Vagotomie ist assoziiert mit schweren Entzündungen, was zu einem hypoxischen Zustand führt, gezeigt durch die Erhöhung der HIF-2α Werte. Die

Ergebnisse von Vagotomie und Vagusnerv-Stimulation unterstützen sogar die Hypothese von Tracey eines "cholinergen entzündungshemmenden Wegs".

Zum Schluss kann gesagt werden, dass die Vagusnerv-Stimulation vor zerebralem Mikrozirkulationsversagen schützt, welches die neuronale Integrität gefährdet. Zudem ist anzumerken, dass die Vagusnerv-Stimulation keinem Effekt auf das NO-System hat.

7. ABBREVIATIONS

°C	Centigrade
ΔΔCt	Delta-delta Ct
%	Percent
ACCP	American College of Chest Physicians
Ach	Acetylcholine
A. femoralis	Arteria femoralis
ANS	Autonomic nervous system
APS	Ammonium persulfate
ATP	Adenosine triphosphate
AV	Atrioventricular
bp	Base pairs
BP	Blood pressure
BSA	Bovine serum albumin
CBF	Cerebral blood flow
cDNA	Complementary deoxyribonucleic acid
ccm	Cubic centimeter
CLP	Cecal ligation and puncture
cm	Centimeter
CMRglc	Cerebral metabolic rate of glucose
CNS	Central nervous system
Ct	Threshold cycle
DIC	Disseminated intravascular coagulation
dl	Deciliter
DMSO	Dimethyl sulfoxide
dNTP	Deoxyribonucleotide triphosphate
DSM	Diagnostic and Statistical Manual
E.coli	Escherichia coli
EEG	Electroencephalogram
EFVR	Evoked flow velocity responses
eNOS	Endothelium nitric oxide synthase
EP	Evoked potential
ER	Endoplasmic reticulum

fMRI	Functional magnetic resonance imaging
FasL	Fas ligand
g	Gram
GAPDH	Glyceraldehyde 3-phosphate dehydrogenase
h	Hour(s)
Hz	Hertz
ICU	Intensive Care Unit
IFN-ɣ	Interferon-ɣ
IL	Interleukin
iNOS	Inducible nitric oxide synthase
i.v.	Intravenous
kDa	Kilo Dalton
kg	Kilogram
L	Liter
lCBF	Local cerebral blood flow
LDF	Laser-Doppler-Flowmetry
LPS	Lipopolysaccharide
µg	Microgram
min	Minute
µl	Microliter
µm	Micrometer
µM	Micromolar
M	Molar
mA	Milliampere
mg	Milligram
ml	Milliliter
mm^3	Cubic Millimeter
mM	Millimolar
Mmol	Millimol
min	Minute
mm	Millimeter
mmHg	Millimeter of mercury
ms	Milliseconds

MEG	Magnetoencephalogram
MHC	Major Histocompatibility complex
MODS	Multiple Organ Dysfunction Syndrome
N	Newton
NaCl	Sodium chloride
N. femoralis	Nervus femoralis
NF-κB	Nuclear factor kappa-light-chain-enhancer of activated B cells
nl	Nanoliter
NLRs	Nod-like receptors
nm	Nanometer
nM	Nanomolar
N_2O	Nitrous oxide
NO	Nitric oxide
NOS	Nitric oxide synthase
n.s	Not significant
PO_2	Partial oxygen pressure
$PaCO_2$	Partial pressure of carbon dioxide
PAGE	Polyacrylamide gel electrophoresis
PAF	Platelet-activating factor
PBGD	Porphobilinogen deaminase
PBS	Phosphate-buffered saline
PCR	Polymerase chain reaction
PIRO	Predisposition Infection Response and Organ Dysfunction
PEEP	Positive Endexpiratory Pressure
PGE	Prostaglandine
PMN	Polymorphonuclear
PMSF	Phenylmethylsulfonyl fluoride
PNS	Peripheral nervous system
PRRs	Pattern recognition receptors
qRT-PCR	Quantitative real time-polymerase chain reaction
rCBF	Regional cerebral blood flow
RLRs	RIG-I (retinoic acid-inducible gene-I)-like receptors
RNA	Ribonucleic acid
Rpm	Revolution per minute

RT-PCR	Reverse transcriptase-polymerase chain reaction
s	Seconds
SCCM	Society of Critical Care Medicine
SD	Standard deviation
SAD	Sepsis-associated delirium
SDS	Sodium dodecyl sulfate
SEP	Somatosensory evoked potential
SIRS	Systemic inflammatory response syndromes
TBST	Tris-buffered saline buffer+ 0.1% Tween 20
TC cells	T cytotoxic cells
TH cells	T helper cells
TEMED	*N*,*N*′,*N*′-tetramethyl-ethane-1,2-diamine
TLRs	Toll-like receptors
TNF-α	Tumor necrosis factor α
Tris	Tris-(hydroxy methyl)-amino methane APS 10% (w/v)
TS cells	T suppressor cells
V	Volt
V. femoralis	Vena femoralis
VGX	Bilateral vagotomy
VGX+STIM	Bilateral vagotomy and distal vagus nerve stimulation
vs.	Versus
WBC	White blood cell

8. LIST OF FIGURES

9. LIST OF TABLES

10. REFERENCES

Abd El-Gawad, H. M. and A. E. Khalifa (2001). "Quercetin, coenzyme Q10, and L-canavanine as protective agents against lipid peroxidation and nitric oxide generation in endotoxin-induced shock in rat brain." Pharmacol Res 43(3): 257-263.

Altavilla, D., S. Guarini, et al. (2006). "Activation of the cholinergic anti-inflammatory pathway reduces NF-kappab activation, blunts TNF-alpha production, and protects againts splanchic artery occlusion shock." Shock 25(5): 500-506.

Angus, D. C., W. T. Linde-Zwirble, et al. (2001). "Epidemiology of severe sepsis in the United States: analysis of incidence, outcome, and associated costs of care." Crit Care Med 29(7): 1303-1310.

Arezzo, J. C., R. Simson, et al. (1985). "Evoked potentials in the assessment of neurotoxicity in humans." Neurobehav Toxicol Teratol 7(4): 299-304.

Ashwal, S., B. Tone, et al. (1998). "Core and penumbral nitric oxide synthase activity during cerebral ischemia and reperfusion." Stroke 29(5): 1037-1046; discussion 1047.

Backer, D. d. (2006). "Lactic Acidosis in Critically Ill Septic Patients." "Sepsis" Ortiz-Ruiz Guillermo Springer Science: 126-133.

Baumane, L., M. Dzintare, et al. (2002). "Increased synthesis of nitric oxide in rat brain cortex due to halogenated volatile anesthetics confirmed by EPR spectroscopy." Acta Anaesthesiol Scand 46(4): 378-383.

Bernik, T. R., S. G. Friedman, et al. (2002). "Cholinergic antiinflammatory pathway inhibition of tumor necrosis factor during ischemia reperfusion." J Vasc Surg 36(6): 1231-1236.

Berthoud, H. R. (2008). "The vagus nerve, food intake and obesity." Regul Pept 149(1-3): 15-25.

Bogdanski, R., M. Blobner, et al. (1999). "[Septic encephalopathy]." Anasthesiol Intensivmed Notfallmed Schmerzther 34(3): 123-130.

Boldt, J. (2002). "Clinical review: hemodynamic monitoring in the intensive care unit." Crit Care 6(1): 52-59.

Bolton, C. F., G. B. Young, et al. (1993). "The neurological complications of sepsis." Ann Neurol 33(1): 94-100.

Bone, R. C., R. A. Balk, et al. (1992). "Definitions for sepsis and organ failure and guidelines for the use of innovative therapies in sepsis. The ACCP/SCCM Consensus Conference Committee. American College of Chest Physicians/Society of Critical Care Medicine." Chest 101(6): 1644-1655.

Borovikova, L. V., S. Ivanova, et al. (2000). "Role of vagus nerve signaling in CNI-1493-mediated suppression of acute inflammation." Auton Neurosci 85(1-3): 141-147.

Borovikova, L. V., S. Ivanova, et al. (2000). "Vagus nerve stimulation attenuates the systemic inflammatory response to endotoxin." Nature 405(6785): 458-462.

Brack, K. E., V. H. Patel, et al. (2009). "Direct evidence of nitric oxide release from neuronal nitric oxide synthase activation in the left ventricle as a result of cervical vagus nerve stimulation." J Physiol 587(Pt 12): 3045-3054.

Comim, C. M., G. T. Rezin, et al. (2008). "Mitochondrial respiratory chain and creatine kinase activities in rat brain after sepsis induced by cecal ligation and perforation." Mitochondrion 8(4): 313-318.

Cox, S. B., T. A. Woolsey, et al. (1993). "Localized dynamic changes in cortical blood flow with whisker stimulation corresponds to matched vascular and neuronal architecture of rat barrels." J Cereb Blood Flow Metab 13(6): 899-913.

Daubin, C., D. Guillotin, et al. (2008). "A clinical and EEG scoring system that predicts early cortical response (N20) to somatosensory evoked potentials and outcome after cardiac arrest." BMC Cardiovasc Disord 8: 35.

De Backer, D., J. Creteur, et al. (2002). "Microvascular blood flow is altered in patients with sepsis." Am J Respir Crit Care Med 166(1): 98-104.

de Jonge, W. J., E. P. van der Zanden, et al. (2005). "Stimulation of the vagus nerve attenuates macrophage activation by activating the Jak2-STAT3 signaling pathway." Nat Immunol 6(8): 844-851.

Devine, S. A., S. M. Kirkley, et al. (2002). "MRI and neuropsychological correlates of carbon monoxide exposure: a case report." Environ Health Perspect 110(10): 1051-1055.

Dirnagl, U., B. Kaplan, et al. (1989). "Continuous measurement of cerebral cortical blood flow by laser-Doppler flowmetry in a rat stroke model." J Cereb Blood Flow Metab 9(5): 589-596.

Dreier, J. P., K. Korner, et al. (1995). "Nitric oxide modulates the CBF response to increased extracellular potassium." J Cereb Blood Flow Metab 15(6): 914-919.

Dyson, A., A. Rudiger, et al. (2011). "Temporal changes in tissue cardiorespiratory function during faecal peritonitis." Intensive Care Med 37(7): 1192-1200.

Dyson, A. and M. Singer (2009). "Animal models of sepsis: why does preclinical efficacy fail to translate to the clinical setting?" Crit Care Med 37(1 Suppl): S30-37.

Ebersoldt, M., T. Sharshar, et al. (2007). "Sepsis-associated delirium." Intensive Care Med 33(6): 941-950.

Engel, C., F. M. Brunkhorst, et al. (2007). "Epidemiology of sepsis in Germany: results from a national prospective multicenter study." Intensive Care Med 33(4): 606-618.

Eyenga, P., F. Lhuillier, et al. (2010). "Time course of liver nitric oxide concentration in early septic shock by cecal ligation and puncture in rats." Nitric Oxide 23(3): 194-198.

Fisher, C. J., Jr. and S. B. Yan (2000). "Protein C levels as a prognostic indicator of outcome in sepsis and related diseases." Crit Care Med 28(9 Suppl): S49-56.

Freeman, B. N. P., Ralph D (2008). "Neurovascular coupling." Scholarpedia 3: 5340.

Gamero, A. M, David M. Reynolds, et al. (2006). "Interferon ɣ: Gene and Protein Structure,Transcription Regulation, and Actions." "The Interferons: Characterization and Application"(Wiley-VCH): 85-110.

Gorg, B., H. J. Bidmon, et al. (2006). "Inflammatory cytokines induce protein tyrosine nitration in rat astrocytes." Arch Biochem Biophys 449(1-2): 104-114.

Guarini, S., D. Altavilla, et al. (2003). "Efferent vagal fibre stimulation blunts nuclear factor-kappaB activation and protects against hypovolemic hemorrhagic shock." Circulation 107(8): 1189-1194.

Hagler, D. J., Jr., E. Halgren, et al. (2009). "Source estimates for MEG/EEG visual evoked responses constrained by multiple, retinotopically-mapped stimulus locations." Hum Brain Mapp 30(4): 1290-1309.

Harve, H., M. Tiainen, et al. (2007). "The functional status and perceived quality of life in long-term survivors of out-of-hospital cardiac arrest." Acta Anaesthesiol Scand 51(2): 206-209.

Hossmann, K. A. (1994). "Viability thresholds and the penumbra of focal ischemia." Ann Neurol 36(4): 557-565.

Hotchkiss, R. S., C. M. Coopersmith, et al. (2009). "The sepsis seesaw: tilting toward immunosuppression." Nat Med 15(5): 496-497.

Howell, M. D., D. Talmor, et al. (2011). "Proof of principle: the predisposition, infection, response, organ failure sepsis staging system." Crit Care Med 39(2): 322-327.

Iadecola, C. (1993). "Regulation of the cerebral microcirculation during neural activity: is nitric oxide the missing link?" Trends Neurosci 16(6): 206-214.

Imtiyaz, H. Z., E. P. Williams, et al. (2010). "Hypoxia-inducible factor 2alpha regulates macrophage function in mouse models of acute and tumor inflammation." J Clin Invest 120(8): 2699-2714.

Iwashyna, T. J., E. W. Ely, et al. (2010). "Long-term cognitive impairment and functional disability among survivors of severe sepsis." JAMA 304(16): 1787-1794.

Kindt, T., B. Osborne, et al (2000). "Kuby Immunology." 6: 4-12.

Klabunde, R. (2011). "Neurohumoral control of the heart and circulation." Cardiovascular Physiology Concepts Lippincott Williams & Wilkins(2): 118-125.

Kruse, J. A. (2002). "Blood lactate concentrations in sepsis." "The sepsis text" Vincent J. L, Jean Carlet,Steven M. Opal Springer: 323-338.

Kumar, H., T. Kawai, et al. (2009). "Pathogen recognition in the innate immune response." Biochem J 420(1): 1-16.

Kuschinsky, W. (1991). "Coupling of function, metabolism, and blood flow in the brain." Neurosurg Rev 14(3): 163-168.

Kuschinsky, W., M. Wahl, et al. (1972). "Perivascular potassium and pH as determinants of local pial arterial diameter in cats. A microapplication study." Circ Res 31(2): 240-247.

Le Cras, T. D. and I. F. McMurtry (2001). "Nitric oxide production in the hypoxic lung." Am J Physiol Lung Cell Mol Physiol 280(4): L575-582.

Lee, C. C., N. T. Lin, et al. (2005). "Inducible nitric oxide synthase inhibition potentiates multiple organ dysfunction induced by endotoxin in conscious rats." J Cardiovasc Pharmacol 45(5): 396-403.

Lehr, HA., F. Bittinger,et al. (2000). "Microcirculatory dysfunction in sepsis: a pathogenetic basis for therapy?" J Pathol 190(3): 373-386.

Lindauer, U., D. Megow, et al. (1999). "Nitric oxide: a modulator, but not a mediator, of neurovascular coupling in rat somatosensory cortex." Am J Physiol 277(2 Pt 2): H799-811.

Linehan, J. D., G. Kolios, et al. (2005). "Effect of corticosteroids on nitric oxide production in inflammatory bowel disease: are leukocytes the site of action?" Am J Physiol Gastrointest Liver Physiol 288(2): G261-267.

Lundy, D. J. and S. Trzeciak (2009). "Microcirculatory dysfunction in sepsis." Crit Care Clin 25(4): 721-731, viii.

Maier, S. F., L. E. Goehler, et al. (1998). "The role of the vagus nerve in cytokine-to-brain communication." Ann N Y Acad Sci 840: 289-300.

Martin, G. S., D. M. Mannino, et al. (2003). "The epidemiology of sepsis in the United States from 1979 through 2000." N Engl J Med 348(16): 1546-1554.

Messaris, E., N. Memos, et al. (2004). "Time-dependent mitochondrial-mediated programmed neuronal cell death prolongs survival in sepsis." Crit Care Med 32(8): 1764-1770.

Minnich, D. J. and L. L. Moldawer (2004). "Anti-cytokine and anti-inflammatory therapies for the treatment of severe sepsis: progress and pitfalls." Proc Nutr Soc 63(3): 437-441.

Mirabella, G., S. Battiston, et al. (2001). "Integration of multiple-whisker inputs in rat somatosensory cortex." Cereb Cortex 11(2): 164-170.

Morris, S. M., Jr. and T. R. Billiar (1994). "New insights into the regulation of inducible nitric oxide synthesis." Am J Physiol 266(6 Pt 1): E829-839.

Müller-Werdan U , S. H. (2005). "Sepsismarker,Sepsismonitoring,Verlaufsbeurteilung der Sepsis." "Sepsis and MODS"(Springer Verlag Heidelberg): 63-77.

Nakao, Y., Y. Itoh, et al. (2001). "Effects of anesthesia on functional activation of cerebral blood flow and metabolism." Proc Natl Acad Sci U S A 98(13): 7593-7598.

Oberholzer, C., A. Oberholzer, et al. (2001). "Apoptosis in sepsis: a new target for therapeutic exploration." FASEB J 15(6): 879-892.

Ohnesorge, H., P. Bischoff, et al. (2003). "Somatosensory evoked potentials as predictor of systemic inflammatory response syndrome in pigs?" Intensive Care Med 29(5): 801-807.

Okamoto, H., O. Ito, et al. (1998). "Role of inducible nitric oxide synthase and cyclooxygenase-2 in endotoxin-induced cerebral hyperemia." Stroke 29(6): 1209-1218.

Okamoto, I., M. Abe, et al. (2000). "Evaluating the role of inducible nitric oxide synthase using a novel and selective inducible nitric oxide synthase inhibitor in septic lung injury produced by cecal ligation and puncture." Am J Respir Crit Care Med 162(2 Pt 1): 716-722.

Papadopoulos, M. C., D. C. Davies, et al. (2000). "Pathophysiology of septic encephalopathy: a review." Crit Care Med 28(8): 3019-3024.

Pullamsetti, S. S., D. Maring, et al. (2006). "Effect of nitric oxide synthase (NOS) inhibition on macro- and microcirculation in a model of rat endotoxic shock." Thromb Haemost 95(4): 720-727.

Rittirsch, D., M. A. Flierl, et al. (2008). "Harmful molecular mechanisms in sepsis." Nat Rev Immunol 8(10): 776-787.

Rivers, E., B. Nguyen, et al. (2001). "Early goal-directed therapy in the treatment of severe sepsis and septic shock." N Engl J Med 345(19): 1368-1377.

Robinson, M. A., J. E. Baumgardner, et al. (2008). "Physiological and hypoxic O2 tensions rapidly regulate NO production by stimulated macrophages." Am J Physiol Cell Physiol 294(4): C1079-1087.

Rosas-Ballina, M. and K. J. Tracey (2009). "The neurology of the immune system: neural reflexes regulate immunity." Neuron 64(1): 28-32.

Rosengarten, B., M. Hecht, et al. (2007). "Microcirculatory dysfunction in the brain precedes changes in evoked potentials in endotoxin-induced sepsis syndrome in rats." Cerebrovasc Dis 23(2-3): 140-147.

Rosengarten, B., M. Hecht, et al. (2008). "Autoregulative function in the brain in an endotoxic rat shock model." Inflamm Res 57(11): 542-546.

Rosengarten, B., H. Lutz, et al. (2003). "A control system approach for evaluating somatosensory activation by laser-Doppler flowmetry in the rat cortex." J Neurosci Methods 130(1): 75-81.

Rosengarten, B., M. Walberer, et al. (2008). "LPS-induced endotoxic shock does not cause early brain edema formation - an MRI study in rats." Inflamm Res 57(10): 479-483.

Rosengarten, B., S. Wolff, et al. (2009). "Effects of inducible nitric oxide synthase inhibition or norepinephrine on the neurovascular coupling in an endotoxic rat shock model." Crit Care 13(4): R139.

Schottmüller (1914). Verhandl dt Kongress Inn Med (31): 257-280

Schuster HP, M. W. (2005). "Definition und Diagnose von Sepsis und Multiorganversagen." "Sepsis and MODS"(Springer Verlag Heidelberg): 4-22.

Seeger, W., F. G., D. Walmrath (2005). "Mediatorblockade und Immunmodulation-Konzeptes und Praxisreifes." "Sepsis and MODS"(Springer Verlag Heidelberg): 249-276.

Semmler, A., T. Okulla, et al. (2005). "Systemic inflammation induces apoptosis with variable vulnerability of different brain regions." J Chem Neuroanat 30(2-3): 144-157.

Sharshar, T., D. Annane, et al. (2004). "The neuropathology of septic shock." Brain Pathol 14(1): 21-33.

Sharshar, T., R. Carlier, et al. (2007). "Brain lesions in septic shock: a magnetic resonance imaging study." Intensive Care Med 33(5): 798-806.

Sjakste, N., J. Sjakste, et al. (2005). "Putative role of nitric oxide synthase isoforms in the changes of nitric oxide concentration in rat brain cortex and cerebellum following sevoflurane and isoflurane anaesthesia." Eur J Pharmacol 513(3): 193-205.

Spanos, A., S. Jhanji, et al. (2010). "Early microvascular changes in sepsis and severe sepsis." Shock 33(4): 387-391.

Spronk, P. E., D. F. Zandstra, et al. (2004). "Bench-to-bedside review: sepsis is a disease of the microcirculation." Crit Care 8(6): 462-468.

Takeda, N., E. L. O'Dea, et al. (2010). "Differential activation and antagonistic function of HIF-{alpha} isoforms in macrophages are essential for NO homeostasis." Genes Dev 24(5): 491-501.

Takeuchi, O. and S. Akira (2010). "Pattern recognition receptors and inflammation." Cell 140(6): 805-820.

Tang, W., J. L. Pakula, et al. (1996). "Adrenergic vasopressor agents and mechanical ventilation for the treatment of experimental septic shock." Crit Care Med 24(1): 125-130.

Tracey, K. J. (2002). "The inflammatory reflex." Nature 420(6917): 853-859.

Tracey, K. J. (2007). "Physiology and immunology of the cholinergic antiinflammatory pathway." J Clin Invest 117(2): 289-296.

Tracey, K. J. (2009). "Reflex control of immunity." Nat Rev Immunol 9(6): 418-428.

Tracy, R. P. (2006). "The Five Cardinal Signs of Inflammation: Calor, Dolor, Rubor, Tumor … and Penuria (Apologies to Aulus Cornelius Celsus, De medicina, c. A.D. 25) " J Gerontol A Biol Sci Med Sci 61(10): 1051-1052.

Trzeciak, S., R. P. Dellinger, et al. (2007). "Early microcirculatory perfusion derangements in patients with severe sepsis and septic shock: relationship to hemodynamics, oxygen transport, and survival." Ann Emerg Med 49(1): 88-98, 98 e81-82.

Ueki, M., G. Mies, et al. (1992). "Effect of alpha-chloralose, halothane, pentobarbital and nitrous oxide anesthesia on metabolic coupling in somatosensory cortex of rat." Acta Anaesthesiol Scand 36(4): 318-322.

van Westerloo, D. J. (2010). "The vagal immune reflex: a blessing from above." Wien Med Wochenschr 160(5-6): 112-117.

Venkatesh, B. and T. J. Morgan (2002). "Monitoring tissue gas tensions in critical illness." Crit Care Resusc 4(4): 291-300.

Vervloet, M. G., L. G. Thijs, et al. (1998). "Derangements of coagulation and fibrinolysis in critically ill patients with sepsis and septic shock." Semin Thromb Hemost 24(1): 33-44.

Vincent, J. L. and D. De Backer (2005). "Microvascular dysfunction as a cause of organ dysfunction in severe sepsis." Crit Care 9 Suppl 4: S9-12.

Vromen, A., M. S. Arkovitz, et al. (1996). "Low-level expression and limited role for the inducible isoform of nitric oxide synthase in the vascular hyporeactivity and mortality associated with cecal ligation and puncture in the rat." Shock 6(4): 248-253.

Wang, K., C. Zheng, et al. (2008). "alpha-Chloralose diminishes gamma oscillations in rat hippocampal slices." Neurosci Lett 441(1): 66-71.

Wray, G. M., C. G. Millar, et al. (1998). "Selective inhibition of the activity of inducible nitric oxide synthase prevents the circulatory failure, but not the organ injury/dysfunction, caused by endotoxin." Shock 9(5): 329-335.

Xu, D., L. Qi, et al. (1993). "Mechanisms of endotoxin-induced intestinal injury in a hyperdynamic model of sepsis." J Trauma 34(5): 676-682; discussion 682-673.

Yale University. Dept. of the History of Science and Medicine and Yale University. Dept. of the History of Medicine. (1946). Journal of the history of medicine and allied sciences. New York, H. Schuman: v.

Zauner, C., A. Gendo, et al. (2002). "Impaired subcortical and cortical sensory evoked potential pathways in septic patients." Crit Care Med 30(5): 1136-1139.

Zheng, H., D. Q. Wei, et al. (2007). "Screening for new agonists against Alzheimer's disease." Med Chem 3(5): 488-493.

Zonta, M., M. C. Angulo, et al. (2003). "Neuron-to-astrocyte signaling is central to the dynamic control of brain microcirculation." Nat Neurosci 6(1): 43-50.

11. PUBLICATIONS

Effects of anti-inflammatory vagus nerve stimulation on the cerebral microcirculation in endotoxinemic rats

Autor: Stanka Mihaylova, Anke Killian, Konstantin Mayer, Soni Savi Pullamsetti, Ralph Theo Schermuly and Bernhard Rosengarten.

Published at 25 July 2012 by Journal of Neuroinflammation

12. ERKLÄRUNG

Erklärung zur Dissertation

„Hiermit erkläre ich, dass ich die vorliegende Arbeit selbständig und ohne unzulässige Hilfe oder Benutzung anderer als der angegebenen Hilfsmittel angefertigt habe. Alle Textstellen, die wörtlich oder sinngemäß aus veröffentlichten oder nichtveröffentlichten Schriften entnommen sind, und alle Angaben, die auf mündlichen Auskünften beruhen, sind als solche kenntlich gemacht. Bei den von mir durchgeführten und in der Dissertation erwähnten Untersuchungen habe ich die Grundsätze guter wissenschaftlicher Praxis, wie sie in der „Satzung der Justus-Liebig-Universität Gießen zur Sicherung guter wissenschaftlicher Praxis“ niedergelegt sind, eingehalten sowie ethische, datenschutzrechtliche und tierschutzrechtliche Grundsätze befolgt. Ich versichere, dass Dritte von mir weder unmittelbar noch mittelbar geldwerte Leistungen für Arbeiten erhalten haben, die im Zusammenhang mit dem Inhalt der vorgelegten Dissertation stehen, und dass die vorgelegte Arbeit weder im Inland noch im Ausland in gleicher oder ähnlicher Form einer anderen Prüfungsbehörde zum Zweck einer Promotion oder eines anderen Prüfungsverfahrens vorgelegt wurde. Alles aus anderen Quellen und von anderen Personen übernommene Material, das in der Arbeit verwendet wurde oder auf das direkt Bezug genommen wird, wurde als solches kenntlich gemacht. Insbesondere wurden alle Personen genannt, die direkt und indirekt an der Entstehung der vorliegenden Arbeit beteiligt waren. Mit der Überprüfung meiner Arbeit durch eine Plagiatserkennungssoftware bzw. ein internetbasiertes Softwareprogramm erkläre ich mich einverstanden.“

_____

_____

Ort, Datum Unterschrift

13. ACKNOLEDGMENTS

I would like to thank Prof. Dr. Kaps for facilitation of this project from 1.12.2009 to 30.11.2012. My deepest gratitude goes first and foremost to my supervisor, Prof. Dr. Bernhard Rosengarten. His professional guidance, constant encouragement, statistical help and support kept me on track during the course of my scientific research.

I sincerely thank Dr. Sabine Klatt for her excellent tutoring during the first 2 months in which I learned the animal experimental procedures. I am also extremely grateful to Prof. Dr. Joachim Roth and Prof. Dr. Schermuly for their cooperative support and intellectual suggestions during this study.

I would like to thank all my wonderful colleagues from group of Prof. Dr. Schermuly for teaching me techniques, offering experimental tips and more important for the nice working atmosphere. To be more specific, I would like to express gratitude to Dr. Xia Tian, Dr. Soni Savai Pullamsetti and Joachim Berk for sharing their experience on real-time PCR and Western blot analysis and friendly support in work as well as in life; to Ewa Bieniek for the help with immunohistochemistry; and also to other colleagues, too numerous to mention, who helped in their own little way throughout this work. A word of appreciation also goes to my colleagues A.Kaschtanov and A.Killian for Elisa analyses. Further I highly appreciate my friends for their kind help and moral support during my study.

“Thank you very much”.

Last but not least, I am especially indebted to my beloved parents and brother for everything they have done for me throughout these years. Without their love and encouragement from them, I can never have the chance to finish my study.